The Plant Cell, Vol. 28: 2326–2341, September 2016, www.plantcell.org

An Autophagy-Related Kinase Is Essential for the Symbiotic Relationship between *Phaseolus vulgaris* and Both Rhizobia and Arbuscular Mycorrhizal Fungi[OPEN]

Georgina Estrada-Navarrete,[a] Neftaly Cruz-Mireles,[a] Ramiro Lascano,[b] Xóchitl Alvarado-Affantranger,[c] Alejandra Hernández-Barrera,[a] Aarón Barraza,[a] Juan E. Olivares,[a] Manoj-Kumar Arthikala,[d] Luis Cárdenas,[a,1] Carmen Quinto,[a] and Federico Sanchez[a,2]

[a] Departamento de Biología Molecular de Plantas, Instituto de Biotecnología, Universidad Nacional Autónoma de México, Cuernavaca, Morelos 62210, Mexico

[b] Centro de Investigaciones Agropecuarias, Instituto de Fisiología y Recursos Genéticos Vegetales, CP 5119 Córdoba, Argentina

[c] Laboratorio Nacional de Microscopía Avanzada, Instituto de Biotecnología, Universidad Nacional Autónoma de México, Cuernavaca, Morelos 62210, Mexico

[d] Escuela Nacional de Estudios Superiores-Unidad León, Universidad Nacional Autónoma de México, León, Guanajuato 37684, Mexico

ORCID IDs: 0000-0002-9576-9941 (R.L.); 0000-0002-3068-2036 (X.A.-A.); 0000-0002-4715-8142 (A.H.-B.); 0000-0002-4535-6524 (M.-K.A.); 0000-0002-6554-5832 (L.C.); 0000-0002-2961-4896 (F.S.)

Eukaryotes contain three types of lipid kinases that belong to the phosphatidylinositol 3-kinase (PI3K) family. In plants and *Saccharomyces cerevisiae*, only PI3K class III family members have been identified. These enzymes regulate the innate immune response, intracellular trafficking, autophagy, and senescence. Here, we report that RNAi-mediated downregulation of common bean (*Phaseolus vulgaris*) *PI3K* severely impaired symbiosis in composite *P. vulgaris* plants with endosymbionts such as *Rhizobium tropici* and *Rhizophagus irregularis*. Downregulation of Pv-*PI3K* was associated with a marked decrease in root hair growth and curling. Additionally, infection thread growth, root-nodule number, and symbiosome formation in root nodule cells were severely affected. Interestingly, root colonization by AM fungi and the formation of arbuscules were also abolished in PI3K loss-of-function plants. Furthermore, the transcript accumulation of genes encoding proteins known to interact with PI3K to form protein complexes involved in autophagy was drastically reduced in these transgenic roots. RNAi-mediated downregulation of one of these genes, *Beclin1/Atg6*, resulted in a similar phenotype as observed for transgenic roots in which Pv-*PI3K* had been downregulated. Our findings show that an autophagy-related process is crucial for the mutualistic interactions of *P. vulgaris* with beneficial microorganisms.

INTRODUCTION

To facilitate the acquisition of nutrients that are not readily available in the soil, most plants establish symbiotic interactions with soil microorganisms such as arbuscular mycorrhizal (AM) fungi of the monophyletic fungal lineage *Glomeromycota* and/or a wide range of gram-negative bacteria, collectively referred to as rhizobia (Bonfante and Genre, 2008; Oldroyd and Downie, 2008). Under stress conditions, the interaction between vascular plants and AM fungi results in an increase in the acquisition of mineral nutrients, particularly phosphate, from the soil by plant roots. By contrast, nitrogen fixation occurs as a consequence of the symbiosis between the roots of legumes and rhizobia. Both of these symbiotic interactions result in the development of de novo structures on the plant roots, namely, arbuscules (intracellular ramified branching hyphae) (Bonfante and Genre, 2008; Parniske, 2008) in the case of mycorrhization and nitrogen-fixing nodules in the case of rhizobial interactions (Oldroyd and Downie, 2008). These mutualistic associations share key evolutionary and developmental features, including a common set of essential plant genes, which are part of the common symbiotic pathway. AM invasion involves the formation of an infection peg from the hyphopodium (specialized fungal cell involved in attachment to the plant host), which mediates fungal hyphal growth into the epidermal cell, and then a prepenetration apparatus, which anticipates the direction of hyphal penetration in the plant cell. Finally, arbuscules arise from the intercellular hyphae in the inner root cortical cells. During nodulation, rhizobia trigger root hair cell curling and infection thread (IT) formation, which allows bacteria to be internalized in the root cortical cells. After reinitiating plant cell division, nodule primordia form. Finally, the IT reaches nodule primordia cells and rhizobia are released and taken up by these cells, which later mature into a functional nitrogen-fixing nodule. Nodulation and mycorrhization rely on Nod and Myc factor signaling, respectively.

The signaling network that underlies these mutualistic interactions has been well studied and is known to involve ionic and cytoskeletal changes (Cárdenas et al., 2000; Oldroyd, 2013).

[1] Address correspondence to luisc@ibt.unam.mx.

[2] In loving memory.

The author responsible for distribution of materials integral to the findings presented in this article in accordance with the policy described in the Instructions for Authors (www.plantcell.org) is: Georgina Estrada-Navarrete (geo@ibt.unam.mx).

[OPEN]Articles can be viewed without a subscription.
www.plantcell.org/cgi/doi/10.1105/tpc.15.01012

Phosphoinositides have been implicated in Nod factor-mediated signaling. However, little is known about the role of phosphoinositides in the modulation of either of these symbiotic interactions (Pingret et al., 1998; Engstrom et al., 2002; Charron et al., 2004; Peleg-Grossman et al., 2007; Xue et al., 2009).

Phosphatidylinositol 3-phosphate (PI3P) is a phosphoinositide that is present at very low levels in plant cells (Brearley and Hanke, 1992). Eukaryotes contain three types of lipid kinases, which belong to the phosphatidylinositol 3-kinase (PI3K) family. In plants and *Saccharomyces cerevisiae*, only PI3K class III family members have been identified. PI3P biosynthesis is catalyzed by PI3K, which is encoded by the only *PI3K* gene reported in *Arabidopsis thaliana*, Vacuolar protein sorting (*Vps34*). PI3P and *PI3K*/*Vps34* are fundamental for normal plant growth and development (Welters et al., 1994; Liu et al., 2005; Lee et al., 2008a, 2008b) and have been implicated in various physiological functions, such as the innate immune response, intracellular trafficking, autophagy, senescence, and the symbiosis of legumes with rhizobia. In soybean (*Glycine max*), two isoforms of PI3K are differentially expressed in roots and nodules. The nodule isoform is highly expressed during nodule organogenesis and has been associated with membrane proliferation (Hong and Verma, 1994). In addition, PI3P mediates the entry of pathogen effector proteins that suppress host defenses and enable disease development during root oomycete infection (Kale et al., 2010). Therefore, PIP3 is an important regulator of the interaction between plants and microbes. Recently, *PI3K* was shown to have an essential role in autophagy (Klionsky and Ohsumi, 1999; Levine and Klionsky, 2004). PI3K/VPS34 interacts with VPS30/BECLIN1 and VPS15 to form a multiprotein complex that functions in autophagy (Kametaka et al., 1998). A novel protein, SH3P2 (SH3 domain protein 2), binds to PI3P downstream of the PI3K complex, which is involved in Arabidopsis autophagosome biogenesis (Zhuang et al., 2013). Autophagy is a highly regulated process in which cytoplasmic materials become enclosed in a double membrane vesicle that is then targeted to the vacuole or lysosome, where the contents are degraded and recycled (Xie et al., 2008). It also plays a central role in processes underlying several physiological responses, including plant development, the innate immune response, and nutrient recycling during starvation and senescence (Hanaoka et al., 2002; Yoshimoto et al., 2004; Liu et al., 2005; Thompson and Vierstra, 2005).

Here, we assessed the functional role of a *Phaseolus vulgaris* PI3K gene during the symbiosis with AM fungi or rhizobia using reverse genetics. Loss of function of Pv-*PI3K* or titration of the PI3P product by overexpression of the FYVE domain drastically inhibited root hair and IT growth and nodule formation, indicating that PI3P is essential for both mycorrhization and nodulation. Furthermore, arbuscule formation with *Rhizophagus irregularis* (formerly known as *Glomus intraradices*) was abrogated upon loss of function of Pv-*PI3K*. Downregulation of Pv-*PI3K* also reduced the transcript levels of autophagy-related genes. RNAi-mediated knocking down of an autophagy-related gene (*Beclin1*/*Atg6*) revealed that autophagy is indeed required for the symbiosis between *P. vulgaris* roots and the soil microorganisms, rhizobia, and AM fungi.

RESULTS

Identification of a *P. vulgaris PI3K* Gene

Using RT-PCR and *Glycine max PI3K*-specific primers (Supplemental Table 1), we amplified a cDNA fragment (847 bp) of *P. vulgaris PI3K* cDNA from total nodule RNA and then used this cDNA fragment as a probe to screen the *P. vulgaris* genomic library. A 13-kb genomic fragment, encoding a PI3K protein of the class III subfamily, was isolated. A BLAST survey of the Phytozome v11 database (http://www.phytozome.net) confirmed that Pv-*PI3K* (ID: Phvul.002G070100.1) is a single-copy gene localized on chromosome 2 and organized in 17 exons and 16 introns. A comparative analysis of *PI3K* genes from monocots and dicots revealed a well conserved *PI3K* gene organization in land plants. The Pv-*PI3K* transcription unit includes 69 and 288 bp of 5′- and 3′-untranslated region, respectively, and an open reading frame encoding a protein of 811 amino acids. In agreement with previously reported PI3K structures, Pv-*PI3K* contains the C2 (Pfam: PF00792) structural domain, which targets proteins to cell membranes; PIK (Pfam: PF00613), also referred to as the HR2 and PI3K accessory domain; and the catalytic domain (Pfam: PF00454), a PI3_PI4 kinase or HR1 domain (Vanhaesebroeck et al., 2010) containing two highly conserved motifs [GDD(I/L)RQD and LGVGDRH] (Herman and Emr, 1990; Hiles et al., 1992; Walker et al., 1999). In pairwise alignments, the Pv-PI3K amino acid sequence exhibited high levels of identity to that of PI3K from Arabidopsis (85%), *Medicago truncatula* (94%), and the root and nodule of *G. max* PI3K isoforms (95%). The phylogenetic tree based on reported PI3K class III amino acid sequences from *P. vulgaris* and other eukaryotes (Supplemental Figure 1; Supplemental Data Set 1) is consistent with the taxonomic order of the organisms included.

Pv-*PI3K* Transcript Levels during the Symbiosis between *P. vulgaris* and *Rhizobium tropici*

In Arabidopsis, *PI3K* is an essential gene that is expressed in almost all tissues, including pollen and root hairs (Welters et al., 1994; Lee et al., 2008a, 2008b). In the roots of 2-d-old *P. vulgaris* seedlings, the relative accumulation of *PI3K* transcript was higher (5.4-fold) in the root hairs, the site of rhizobial entry into the root, and in the root apex (4.1-fold) than in the stripped root (depleted of root hairs) (Figure 1A). To determine the role of Pv-*PI3K* during the *P. vulgaris* symbiosis with bacteria, we evaluated Pv-*PI3K* transcript levels in common bean roots soon after inoculation with *R. tropici* CIAT 899 and in uninoculated roots. No significant differences were observed between samples of *R. tropici*-inoculated and uninoculated roots harvested at 6, 12, 24, 48, or 72 h after inoculation (hai). However, the level of Pv-*PI3K* transcript in roots inoculated with rhizobia was higher at 96 hai (1.41 ± 0.24, SD) than in uninoculated roots (0.49 ± 0.073) and was 2.5-fold higher at 144 hai (3.99 ± 0.56 versus 1.57 ± 0.23) (Figure 1B) than in uninoculated roots. *ENOD40* is an early nodulin gene that is upregulated at the onset of nodulation and therefore considered as a marker of nodule development (Crespi et al., 1994; Kumagai et al., 2006; Blanco et al., 2009; Montiel et al., 2012; Okazaki et al., 2013). A 10.4-fold increase in the transcript levels of Pv-*ENOD40*

in the inoculated roots collected at 72 hai (Figure 1C) confirmed that the molecular mechanisms underlying nodulation had been activated. In nodules collected from roots at 10 to 30 d after inoculation (dai), Pv-*PI3K* transcript levels increased during nodule development and peaked at 22 dai, corresponding to the stage at which nitrogen fixation activity in the nodule is highest (Mylona et al., 1995), and then decreased as the nodule senesced (30 dai; Supplemental Figure 2A). To evaluate the spatiotemporal expression of Pv-*PI3K* during nodule organogenesis, we cloned the Pv-*PI3K* promoter (region ~1 kb directly upstream of the initiation codon) in a transcriptional fusion with the chimeric reporter GFP-GUS to yield *PvPI3K*$_{pro}$*:GFP-GUS*. Pv-*PI3K* promoter activity was therefore monitored as GUS activity or GFP fluorescence in *P. vulgaris* transgenic hairy roots generated by *Agrobacterium rhizogenes* K599-mediated transformation (Estrada-Navarrete et al., 2007). Control transgenic roots harbored a cassette with no promoter sequences upstream of the GFP-GUS sequences. In *P. vulgaris* transgenic roots harboring *PvPI3K*$_{pro}$*:GFP-GUS*, the activity of the Pv-*PI3K* promoter was detected at the tip and in the vascular tissue of the root and in the basal cells of the lateral root primordia (Figures 1D to 1F). *PvPI3K*$_{pro}$*:GFP-GUS* transgenic roots inoculated with *R. tropici* showed a strong GUS signal in the tips, but barely any signal in the vascular tissue adjacent to the infection site (Figures 1G and 1H). The Pv-*PI3K* promoter is highly active in infected root hairs and in cells of the nodule primordia (Figures 1H and 1I).

We next examined Pv-*PI3K* promoter-driven GFP-GUS expression during the early stages of infection in hairy roots inoculated with *R. tropici* expressing the fluorescent marker DsRed using laser scanning confocal microscopy. A representative image of a typical IT (harboring DsRed-expressing rhizobia), growing from the root hair through the GFP-expressing cells of a nodule primordium is shown in Figures 1J to 1L. In the mature nodule (22 dai), the Pv-*PI3K* promoter was mainly active in the central tissue (Supplemental Figure 2B), whereas at 30 dai, the promoter activity was restricted to the nodule vascular bundles (Supplemental Figure 2C). Neither rhizobia-inoculated nor uninoculated control transgenic roots bearing the promoter-less GFP-GUS construct exhibited GUS activity (Figures 1M to 1O; Supplemental Figures 2D to 2K).

Downregulation of *PI3K* Affects Root Hair Growth and Curling in Response to Rhizobia Inoculation

To gain insight into the role of Pv-*PI3K* during nodule organogenesis and AM symbiosis, we used RNAi to knock down the expression of Pv-*PI3K* in *P. vulgaris* composite plants, in which only the hairy roots were transgenic. A specific *PvPI3K*-RNAi construct (537 bp) was cloned downstream of the 35S promoter sequence in the Gateway-based hairpin vector pTdT-DC-RNAi (Valdés-López et al., 2008) to generate pTdT-PvPI3K-RNAi. A previously described construct bearing a truncated and irrelevant sequence from Arabidopsis pre-mir159 cloned in pTdT-DC-RNAi (Montiel et al., 2012) was used as a control vector and is herein referred to as pTdT-*Sac*-RNAi. Transgenic hairy roots were selected based on the expression of red fluorescent protein tdTomato (tandem dimer Tomato; Shaner et al., 2004) encoded by the vector. Nonfluorescent roots were discarded. In individual transgenic roots expressing the Pv-*PI3K*-specific RNAi, the levels of Pv-*PI3K* transcript were reduced by ~60% with respect to the levels found in individual control transgenic roots (Figure 2A; Supplemental Figure 3A).

Loss of function of Pv-*PI3K* did not affect root hair density but had a striking effect on root hair length, possibly indicating that *PvPI3K*-RNAi transgenic roots had a lower proportion of long root hairs at 12 d. This indicates that PI3K has a direct effect on root hair length. However, the maximum length of root hairs in *P. vulgaris* roots is unknown. Data reported by Blanco et al. (2009) showed that root hairs in *P. vulgaris* transgenic roots expressing an irrelevant GUS-RNAi were ~250 ± 80 μm in length (Blanco et al., 2009). To determine the relative length of root hairs in *PvPI3K*-RNAi and control transgenic roots, a series of digital images, representative of root zones presenting a similar density of root hairs, were analyzed (Supplemental Figure 3B). Although it cannot be established whether the root hairs measured were still growing or had ceased to grow, the length of the longest root hairs in control transgenic roots was 402 ± 60 μm, and we used this length as a parameter for length measurements. According to Dolan et al. (1993), Arabidopsis root hairs grow in three discrete, successive phases. After the appearance of small bulges, tip-growing root hairs first grow slowly and then grow more rapidly (Dolan et al., 1993). Based on these phases, *P. vulgaris* transgenic root hair cells were distributed in three groups: bulges or emerging root hairs; short root hairs, having a length equivalent to one-third or less of 402 ± 60 μm (i.e., <130 μm), which may include cells with a slow tip-growing phase that are transitioning to an increasing rate of tip growth; and long root hairs, having a length of >130 μm (Figures 2B to 2D). While no differences were found when comparing the percentage of short root hairs observed in *PvPI3K*-RNAi and control transgenic roots, more bulges were found in *PvPI3K*-RNAi (28.86% ± 4.69%) than in the control (15.37% ± 2.31%) and a decrease of ~2-fold was found in the percentage of long root hairs (14.36% ± 2.60%) in *PvPI3K* loss-of-function transgenic roots with respect to control transgenic roots (33.12% ± 4.36%) (Figure 2F; Supplemental Table 2). Root hair curling, a typical response to the species-specific interaction between the root hair and the rhizobia, was affected by the downregulation of Pv-*PI3K* expression. Only 3.39% ± 1.70% of root hairs in *PvPI3K*-RNAi transgenic roots exhibited curling, compared with 31.30% (±4.20) in transgenic inoculated control roots (72 hai), as shown in Figures 2E and 2G.

Loss of Function of Pv-*PI3K* Impairs Nodule Organogenesis in Transgenic Roots

To assess the effects of the loss of function of Pv-*PI3K* on nodule organogenesis in *P. vulgaris* transgenic roots, we analyzed the events of infection and nodulation after inoculation with *R. tropici* expressing GFP by laser scanning confocal microscopy. At 12 dai, typical ITs formed and ramified in the root hair and further penetrated the dividing cells beneath the infection site in control transgenic roots (Figures 3A, 3B, and 3C). In *PvPI3K*-RNAi transgenic roots, IT growth was arrested at the base of the infected root hair, impairing its progress toward the first dividing cell layer beneath the infection site (Figures 3D to 3F). We then determined how many arrested ITs (AITs) were present in the transgenic roots.

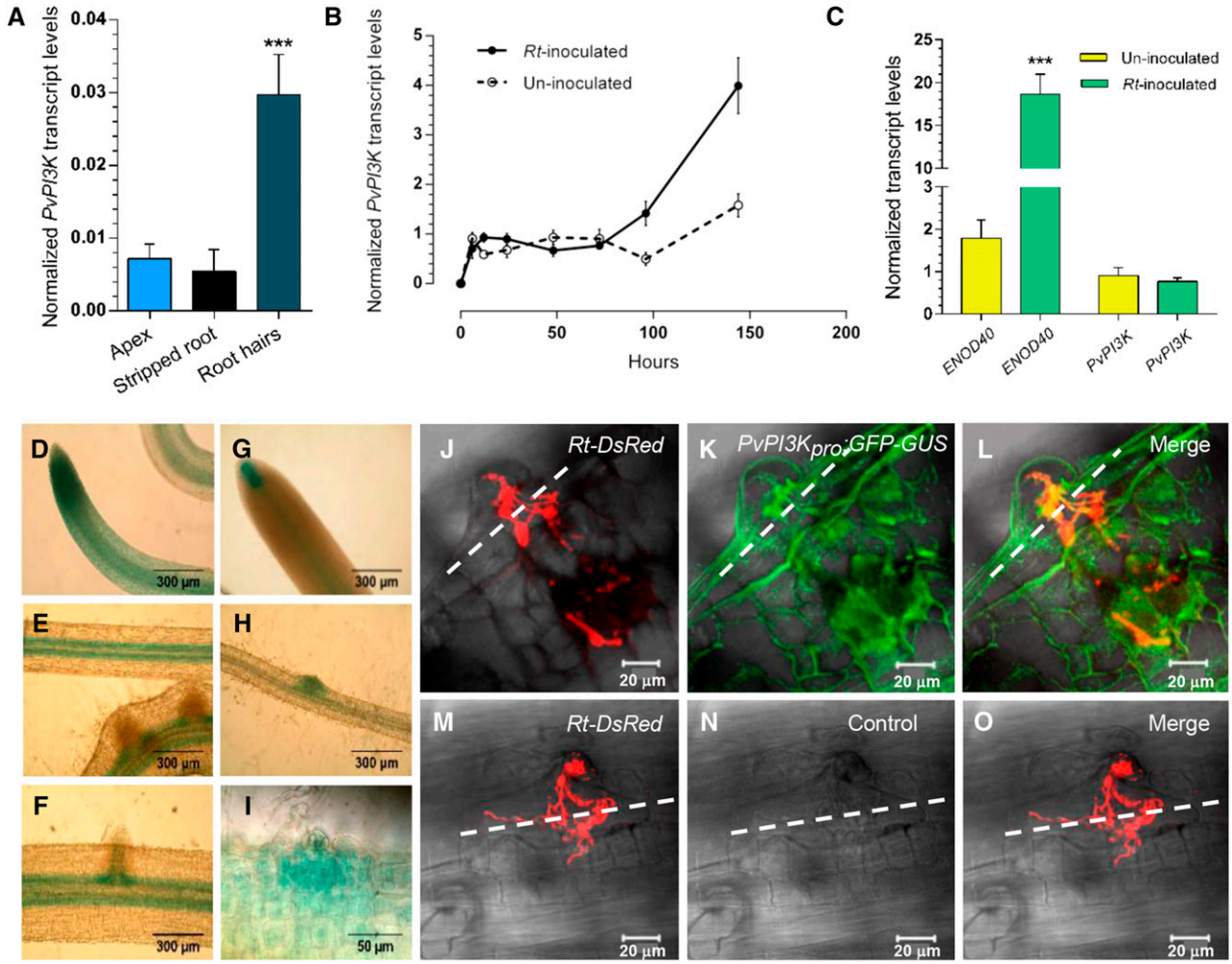

Figure 1. Pv-*PI3K* Transcript Levels and Pv-*PI3K* Promoter Activity during the Early Stages of the Symbiosis between *P. vulgaris* and *R. tropici* CIAT 899.

(A) to **(C)** Quantification of transcript levels by RT-qPCR analysis.

(A) *PI3K* transcript levels were higher in root hairs than in the root apex and stripped roots collected from 2-d-old *P. vulgaris* seedlings. Bars represent the mean and SD (±SD) of two experiments (n = 2 from pool of 150 root tissues of seedlings treated to separate the apex and stripped roots).

(B) The level of Pv-*PI3K* transcript increases in wild-type *P. vulgaris* roots at 96 and 144 hai with *R. tropici* CIAT 899. At 6, 12, 24, 48, and 72 hai, *PvPI3K* transcript levels in inoculated roots were comparable to those in uninoculated roots. Black line, roots inoculated with *R. tropici* CIAT 899; dotted line, uninoculated roots. Bars represent mean ± SD of three experiments (n = 3 from pool of 10 roots).

(C) An increase in Pv-*ENOD40* transcript level in rhizobia-inoculated roots (72 hai) confirmed the activation of nodulation. No significant difference was found in Pv-*PI3K* transcript levels following inoculation. Bars represent mean (±SD) of three experiments (n = 3 from pool of 10 roots).

In **(A)** to **(C)**, transcript levels were quantified by reverse transcription and real-time PCR (RT-qPCR) and calculated using levels of *Elongation Factor 1*α as reference, as described in Methods. Each RNA sample was assessed in triplicate. The number of biological replicates (n) is indicated. Error bars indicate mean and SD (±SD). For **(A)** and **(B)**, statistically significant differences were determined by one-way ANOVA followed by Tukey's test (***$P < 0.0001$). For **(C)**, statistically significant differences were confirmed by an unpaired two-tailed Student's t test (***$P < 0.001$).

In **(D)** to **(I)**, *PvPI3K*$_{pro}$*:GFP-GUS* activity in transgenic roots was detected at the root tip (**[D]** and **[G]**), the vascular tissue **(E)**, and in the cells at the base of lateral root primordia **(F)**, as assessed by GUS staining. When inoculated with *R. tropici* CIAT899, the Pv-*PI3K* promoter was highly active in the infected root hair **(I)** and in the cells adjacent to the infection site **(H)**. Bars = 300 µm in **(D)** to **(H)** and 50 µm in **(I)**.

(J) to **(O)** Hairy roots transformed with *PvPI3K*$_{pro}$*:GFP-GUS* were inoculated with *R. tropici* CIAT899 expressing the fluorescent marker DsRed (*R. tropici*-DsRed). Activity, detected as GFP fluorescence, was observed at the infection site **(K)** and merge in **(L)**. Infection thread progression and ramification were traced by the fluorescence of DsRed (*Rt-DsRed*; red in **[J]** and **[M]**; merge in **[L]**). No green fluorescence was detected in *P. vulgaris* transgenic roots harboring a promoterless construct (control vector; **[N]**). White dashed lines indicate the border between the root epidermis and the adjacent cortical cell layer. Images were acquired in vivo using a Zeiss LSM 510 Meta Confocal Microscope; 21 optical sections each of 0.89 µm were acquired for *PvPI3K*$_{pro}$*:GFP-GUS* roots, and 16 optical sections each of 1.89 µm for the control roots. Transgenic roots were analyzed at 15 dai. Bars = 20 µm.

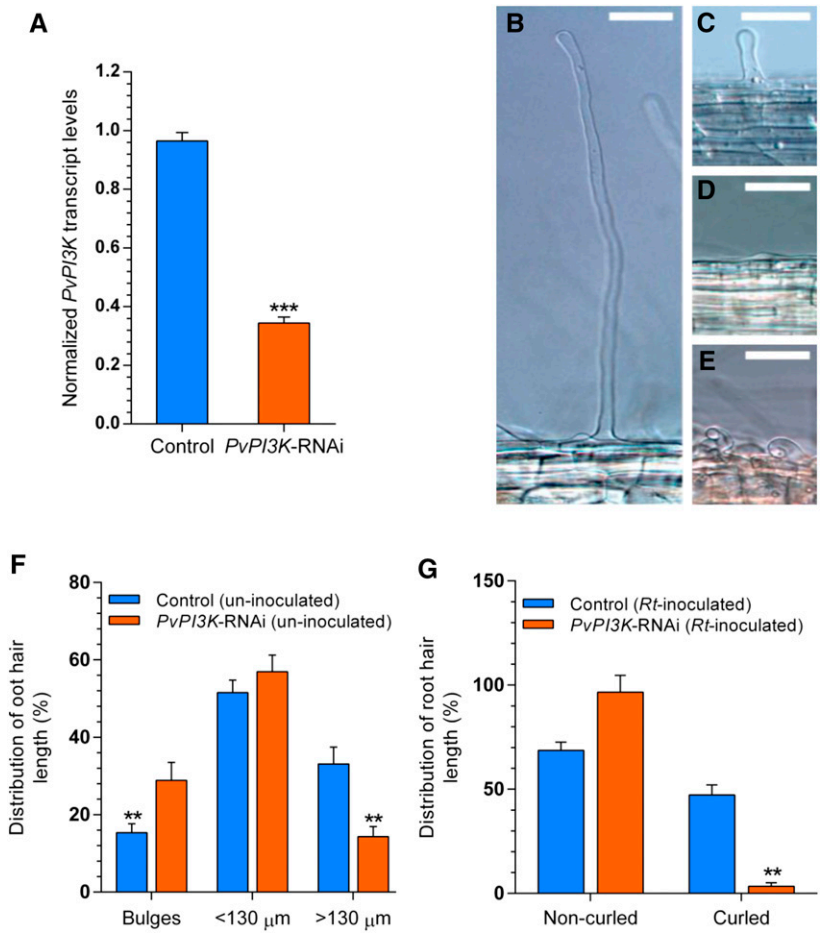

Figure 2. Loss of Function of *Pv*PI3K Inhibits Root Hair Growth and Root Hair Curling after *R. tropici* Inoculation.

(A) The extent of *PvPI3K* downregulation was determined by RT-qPCR analysis in individual red-fluorescent transgenic roots expressing *PvPI3K*-specific RNAi. A comparison between normalized *PvPI3K* transcript levels and control transgenic roots expressing TdT-*Sac*-RNAi. Normalized transcript levels were quantified by RT-qPCR using transcript levels of *Elongation Factor 1α* as reference. Bars are the mean ± SD of four (n = 4) independent transgenic roots (biological replicates), and each sample was analyzed in triplicate. Statistical significance was confirmed by an unpaired two-tailed Student's t test (***P < 0.004).

(B) to **(D)** Representative images of *P. vulgaris* root hairs of different length, as described in this work: long, >130 μm **(B)**; short, <130 μm **(C)**; and emerging root hair or bulge **(D)**. Bars = 50 μm.

(E) Representative image of a *P. vulgaris* curled root hair. Curling is typically observed after root inoculation with *R. tropici* CIAT 899. Bar = 50 μm.

(F) Distribution of root hair length in 12-d-old control (blue bars) and *PvPI3K*-RNAi (orange bars) transgenic roots, presented as percentage (%), where 100% is the sum of all root hairs counted.

(G) Distribution of noncurled and curled root hairs in control (blue bars) and *PvPI3K*-RNAi (orange bars) transgenic roots inoculated with *R. tropici* CIAT 866 and collected at 72 hai. Presented as percentage, where 100% is the sum of curled and noncurled root hairs.

Roots were cleared and root sections of ~3 cm in length were mounted on glass microscope slides as described in Methods. Bars are the mean value (%) of 15 or 16 independent transgenic roots (n = 15 to 16). Bars refer to mean ± SE. Statistically significant differences were confirmed by an unpaired two-tailed Student's t test with Welch's correction (**P < 0.005).

An average of 6.43 ± 0.71 AITs/root were found on *PvPI3K*-RNAi transgenic roots, whereas AITs on control transgenic roots were scarce (0.125 ± 0.03 AITs/root; Figure 3G). Loss of function of Pv-*PI3K* did not seem to affect reinitiation of the cell cycle in the outer cortical cells at the infection site (Figure 3F). This cell activity is a characteristic feature of the determinate type of nodulation, such as that exhibited by *P. vulgaris* (van Spronsen et al., 2001). The roots of control transgenic plants (Figure 3H; Supplemental Figures 4A to 4C) had 218.90 ± 73.40 nodule primordia and 172.40 ± 68.50 nodules per plant. In transgenic roots expressing *PvPI3K*-RNAi, the number of nodule primordia and nodules per plant was drastically reduced (40.66 ± 18.34 and 24.50 ± 14.39 per plant, respectively). Additionally, *PvPI3K*-RNAi nodules were smaller than those produced on control transgenic roots expressing TdT-*Sac*-RNAi (Supplemental Figures 4A and 4B). These data indicate that downregulation of Pv-*PI3K* led to a drastic

reduction in the number of nodule primordia (5-fold) and nodules (7-fold) with respect to control transgenic roots. Another phenotypic feature affected by Pv-*PI3K* loss of function involved infection of cells in the central tissue of the nodule. Almost all cells in the central tissue of nodules generated in control transgenic roots were infected with rhizobia expressing GFP (Supplemental Figure 4D). In the case of *PvPI3K*-RNAi transgenic roots inoculated with *R. tropici*-GFP, the vast majority of the nodules did not contain cells infected with rhizobia-GFP (Supplemental Figure 4E), although ITs exhibiting *R. tropici*-GFP fluorescence were frequently observed at the periphery of the empty nodules, suggesting that the IT remained arrested in the root hair (Supplemental Figure 4F). As expected, the acetylene reduction assessment indicates that nitrogen fixation was barely detected in nodules harvested from *PvPI3K*-RNAi transgenic roots (10.28 ± 2.37 μmol ethylene/h/g of nodule dry weight) when compared with those collected from control transgenic roots (67.20 ± 10.39 μmol ethylene/h/g of nodule dry weight). Therefore, Pv-*PI3K* loss of function not only has an effect on nodule organogenesis, but also impairs nodule infection.

Expression of the FYVE Domain Phenocopies Nodulation Impairment in Loss of Function of Pv-*PI3K* Transgenic Roots

To investigate whether PI3P, the product of Pv-PI3K kinase activity, is required for nodule organogenesis, a fluorescent biosensor (*YFP-2xFYVE*; Vermeer et al., 2006) was transgenically expressed in roots to specifically visualize PI3P in living cells. FYVE zinc finger domains present in four cysteine-rich proteins, i.e., Fab1, YOTB, Vac1, and EEA1 (Stenmark et al., 1996; Gaullier et al., 1998; Patki et al., 1998), were identified as having the ability to direct the highly specific binding of biosensor molecules, such as GFP or YFP, to PI3P in animal cells. A similar strategy was applied to study cowpea (*Vigna unguiculata*) protoplasts, tobacco (*Nicotiana tabacum*) BY-2 cells, and Arabidopsis root epidermal cells and stomata (Vermeer et al., 2006).

P. vulgaris transgenic roots harboring a *2x35S:YFP-2xFYVE* construct and inoculated with DsRed-expressing *R. tropici* were phenotypically similar to transgenic roots in which Pv-*PI3K* expression was downregulated. Although rhizobia interacted with root hairs and ITs formed in transgenic roots expressing YFP-2xFYVE, IT progression was arrested in the root hair, but activation

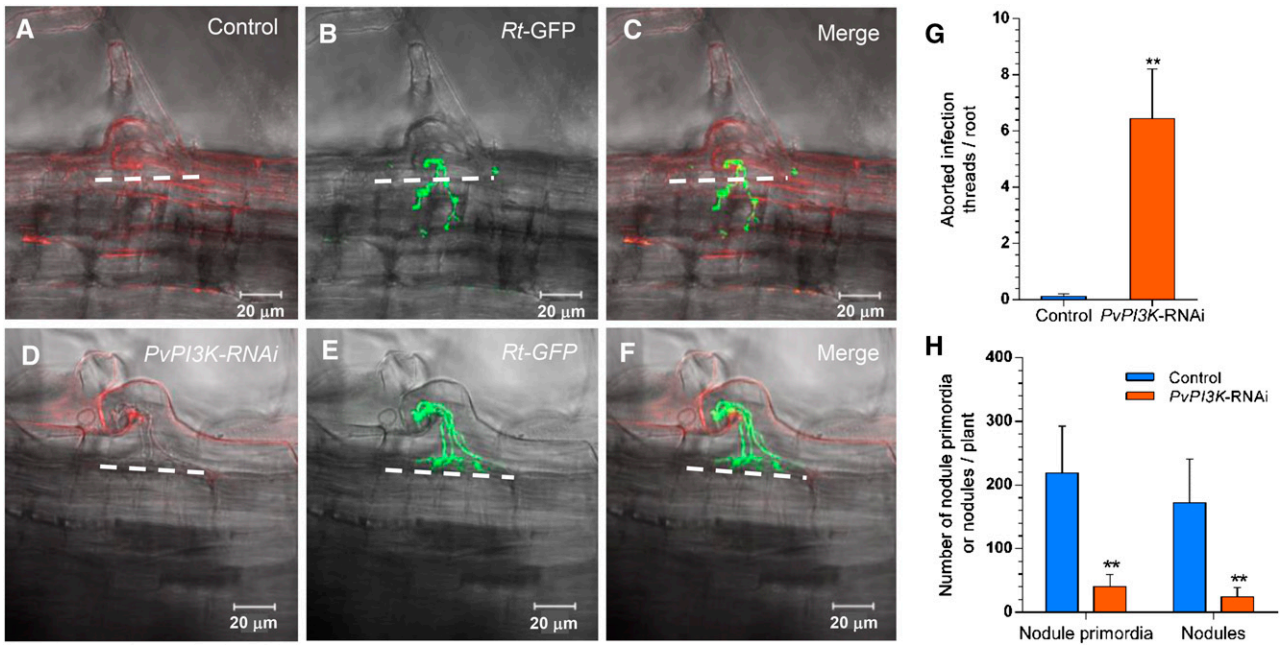

Figure 3. Loss of Function of Pv-*PI3K* Impairs Infection Thread Growth, Ramification, and Nodule Development in *P. vulgaris* Transgenic Roots.

(A) to **(F)** Representative in vivo images of ITs formed in *P. vulgaris* control (**[A]** to **[C]**) and *PvPI3K*-RNAi transgenic roots (**[D]** to **[F]**) inoculated with *R. tropici* CIAT899 expressing GFP (*Rt*-GFP; green) in **(B)** and **(E)**. Control (TdT-*Sac*-RNAi) and *PvPI3K*-RNAi roots expressed the red fluorescent tdTomato reporter marker in **(A)** and **(D)**. Infection thread progression and ramification were traced based on GFP fluorescence. White dashed lines indicate the border between the root epidermis and the adjacent cortical cell layer. In *PvPI3K*-RNAi transgenic roots, IT growth was arrested at the base of the root hair, before entering the dividing cell layers adjacent to the infection site. This IT phenotype is referred to as an arrested or abortive IT (AIT). Images were acquired in vivo using a Zeiss LSM 510 Meta Confocal Microscope; 34 optical sections (1.0 μm) were acquired for the control and 27 optical sections (1.0 μm) for the *PvPI3K*-RNAi roots. Bars = 20 μm.

(G) More AITs were formed on the *PvPI3K*-RNAi transgenic roots than on the control (TdT-*Sac*-RNAi) transgenic roots. Bars represent the mean ± SD of AITs/root of independent transgenic roots (n = 16). Asterisks indicate statistically significant difference (unpaired two-tailed Student's t test, **P < 0.05).

(H) The numbers of nodule primordia and nodules were reduced in Pv-*PI3K*-downregulated transgenic roots with respect to control transgenic roots. Bars represent mean ± SD (n = 10 transgenic roots from composite plants; 22 dai). Asterisks indicate statistically significant difference (unpaired two-tailed Student's t test, **P < 0.003 and **P < 0.05, respectively).

of the cell cycle in cortical cells adjacent to the infection site was not affected. Multiple AITs were often observed within the same root hair (Figures 4A to 4C). Neither IT elongation toward the dividing cortical cells (Figures 4D to 4F) nor the nodule number was affected in control transgenic roots bearing a 35S-YFP construct (Figure 4G). A reduction in the number of nodules of ~5-fold was associated with the expression of the biosensor YFP-2xFYVE (Figure 4G). In summary, these data indicate that the expression of the PI3P binding biosensor YFP-2xFYVE mimics the loss of function of Pv-*PI3K* and strongly suggest that the catalytic activity of Pv-PI3K is instrumental for nodulation in *P. vulgaris.*

Autophagy Is Downregulated in Pv-*PI3K* Loss of Function *P. vulgaris* Roots

VPS34/PI3K, VPS15 (the regulatory subunit) and the accessory proteins VPS30/BECLIN1 and ATG14 form a protein multicomplex that is required for autophagy in yeast (Stack and Emr, 1993; Stack et al., 1995; Kametaka et al., 1998; Kihara et al., 2001). Whereas no *Atg14* ortholog was found in plants (Levine and Klionsky, 2004), *Vps15* and *Beclin1* of this complex had orthologs in plants. To gain insight into the expression of Pv-*Vps15*, Pv-*Beclin1*, and the autophagy universal marker Pv-*Atg8* in *P. vulgaris*, we performed a comparative analysis of the transcript accumulation of these genes in roots expressing *PvPI3K*-RNAi. The transcript level of *PI3K* in roots expressing *PvPI3K*-RNAi was decreased by 66.3% ± 2.3% relative to control (TdT-*Sac*-RNAi) roots. A 79.4% ± 2.28% decrease in the abundance of Pv-*Vps15* transcript was found in Pv-*PI3K* loss-of-function transgenic roots. A statistically significant reduction was also found in the transcript accumulation patterns of Pv-*Beclin1* (59% ± 3.4%) and Pv-*Atg8* (32.1% ± 9.2%), as shown in Figure 5.

An Arabidopsis *Beclin1*-deficient mutant (*beclin1*) exhibits pollen germination defects, dwarfism, and early senescence. Genes involved in phosphatidylinositol metabolism and signaling and the glycosyl phosphatidyl inositol) anchor system are also significantly disrupted in *bcl1* plants (Qin et al., 2007). *Nicotiana benthamiana Beclin1* is essential for restriction of the hypersensitive response and programmed cell death (Liu et al., 2005). In an attempt to evaluate the functional relationship between Pv-*PI3K* and Pv-*Beclin1* during nodule organogenesis, we generated a *PvBeclin1*-RNAi construct. Pv-*Beclin1* transcript levels were reduced by 78.68% ± 2.74% in roots expressing *PvBeclin1*-RNAi compared with control transgenic roots (Figure 6A). The roots of plants in which Pv-*Beclin1* expression was downregulated had far fewer nodules (11.2 ± 3.9) than did control roots expressing the TdT-*Sac*-RNAi (239.3 ± 34.2) at 21 dai with *R. tropici* (Figure 6B).

Pv-*PI3K* Transcript Levels and Promoter Activity in *P. vulgaris* Roots after Inoculation with *R. irregularis*

To address the participation of Pv-*PI3K* in the AM symbiosis in common bean roots, 5-d-old wild-type *P. vulgaris* seedlings were inoculated with *R. irregularis* and examined at 3 and 6 weeks after inoculation (wai). Uninoculated plants grown under identical conditions were used as controls. Fungal colonization was confirmed by Trypan blue staining and monitored by RT-qPCR measurement of *P. vulgaris* phosphate-transporter T4 (*PvPT-4*) transcripts, an indicator of progressive colonization (McGonigle et al., 1990; Arthikala et al., 2013). As expected, the relative levels

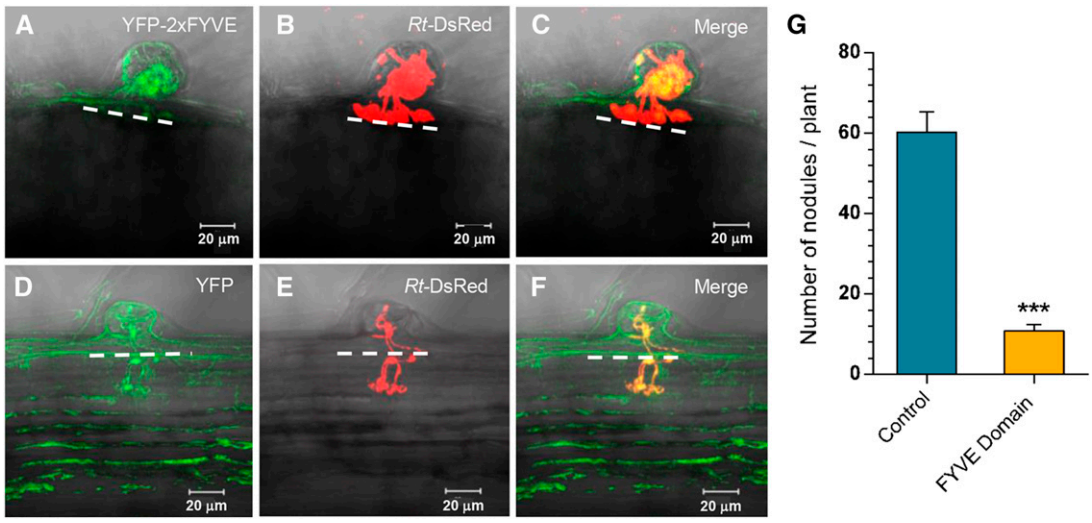

Figure 4. Expression of the FYVE Domain Phenocopies the Loss of Function of Pv-*PI3K* in *P. vulgaris* Transgenic Roots after *R. tropici* Inoculation.

(A) to **(F)** Transgenic roots expressing YPF-2xFYVE or YFP (control) were inoculated with *R. tropici*-DsRed and fluorescence was observed in vivo at 15 dai by confocal microscopy. Representative images of an infection site in YPF-2xFYVE expressing roots revealed that IT progression was arrested **(A)** and ITs fail to reach the first cell layer of the outer cortex (**[B]** and **[C]**). A typical IT progression was observed in control transgenic roots (**[D]** to **[F]**). Images were acquired in vivo using a Zeiss LSM 510 Meta Confocal Microscope, and 23 optical sections each of 0.89 μm were acquired for YFP-2xFYVE and 25 optical sections each of 1.0 μm for the control roots. Bars = 20 μm.

(G) Fewer nodules were produced by transgenic roots expressing YPF-2xFYVE than by control transgenic roots (expressing YFP). Bars represent mean ± SD (n = 10 composite plants; 21 dai). Asterisks indicate statistically significant differences (unpaired two-tailed Student's t test, ***P < 0.006).

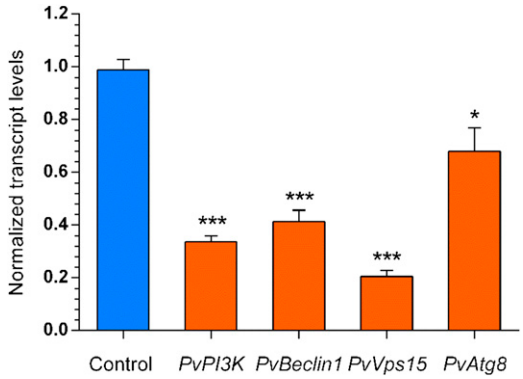

Figure 5. Transcript Accumulation Analysis Showed That the Autophagy Genes Pv-*Beclin1*, Pv-*Vps15*, and Pv-*Atg8* Were Downregulated upon Pv-*PI3K* Loss of Function.

RNA samples from *P. vulgaris PvPI3K*-RNAi transgenic roots with a reduction in Pv-*PI3K* transcript levels (~66%) were further assessed by RT-qPCR analysis to quantify the transcript levels of Pv-*Beclin1*, Pv-*Vps15*, and Pv-*Atg8*. Calculations of normalized transcript level were made using *Elongation Factor 1α* as reference gene, as described in Methods. Bars refer to mean ± SD of two experiments ($n = 2$ from pools of 8 transgenic roots, biological replicates; each RNA sample was analyzed in triplicate). Statistically significant differences were determined using an unpaired two-tailed Student's *t* test (*P < 0.05 and ***P < 0.001).

of *PvPT-4* transcript increased in response to *R. irregularis* inoculation, whereas no significant changes were observed in Pv-*PI3K* transcript levels between roots colonized with AM fungi and control uninoculated roots (Figures 7A and 7B).

Although the AM symbiosis in *P. vulgaris* has not been characterized in the same level of detail as in *M. truncatula* (Genre et al., 2008), a previous report described the key stages of AM infection in *P. vulgaris* roots (Arthikala et al., 2013). To survey the spatio-temporal Pv-*PI3K* promoter activity upon *R. irregularis* inoculation of transgenic roots harboring the construct *PvPI3K*$_{pro}$*:GFP-GUS*, we harvested the roots at 3 wai. *R. irregularis* was stained with an Alexa Fluor 633 conjugated to wheat germ agglutinin (WGA), which exhibits far-red fluorescence (Arthikala et al., 2013). Pv-*PI3K* promoter activity, revealed as GFP fluorescence, was restricted to epidermal cells (Figure 7D) neighboring the contact point of the fungal hyphae (Figures 7C and 7E, merge) and to those beneath the expanding extraradical hyphae (Figures 7F to 7H, merge). However, no PPA-like structures were detected, suggesting that the Pv-*PI3K* promoter was active prior to the formation of the PPA. The later stages of AM infection in cortical cell layers could not be analyzed due to the thickness of *P. vulgaris* transgenic roots beyond 3 wai.

Pv-*PI3K* Loss of Function Impairs AM Symbiosis

We next examined whether Pv-*PI3K* is required for the AM symbiosis in *PvPI3K*-RNAi transgenic roots (3 wai) stained with Trypan blue. As observed in Figure 8A, control transgenic roots showed a typical AM colonization pattern, which includes epidermal penetration by the fungal partner, formation of intracellular apoplastic compartments, ramification, and fungal colonization of both the outer and inner cortex with abundant arbuscules. All fungal structures were identified, namely, extraradical and intraradical hyphae, hyphopodium, and arbuscules with trunks and branches (Figure 8A). By contrast, typical mycorrhizal infection was drastically impaired in *PvPI3K*-RNAi transgenic roots. An increased number of extraradical hyphae and hyphopodia that seem to be arrested at the fungal contact site were observed with respect to control transgenic roots expressing TdT-*Sac*-RNAi (Figure 8B). Furthermore, finger-like outgrowths (10.90 ± 1.13/root) were often observed in extracellular hyphae in the down-regulated transgenic roots (Figures 8C to 8E; Supplemental Figure 5A), whereas such structures were barely detected in control transgenic roots (less than one/root; Figure 8A; Supplemental Figure 5B). Occasionally, intraradical hyphae were found to penetrate the outer cortex (Figure 8B), but intracellular infection and arbuscule formation in the epidermis and outer cortex were never observed. To estimate the effect of Pv-*PI3K* downregulation on the extent of AM fungal colonization, we quantified the overall percentage of root length colonization (%RLC) (McGonigle et al., 1990) at 3 and 6 wai in control and *PvPI3K*-RNAi transgenic roots inoculated with *R. irregularis*. In *PvPI3K*-RNAi transgenic roots, an AM fungal colonization percentage of 7 ± 1.2 and 11.16 ± 3.5% RLC was observed at 3 and 6 wai, respectively, which represents about a 5.25-fold reduction with respect to control transgenic roots (i.e., 41.50 ± 2.0 and 65.0 ± 5.0%RLC at 3 and 6 wai, respectively; Figure 8F). Transcriptional activation of Pv-*PT-4*, a molecular tracker of AM colonization, was also impaired in *PvPI3K*-RNAi transgenic roots inoculated with *R. irregularis*. As

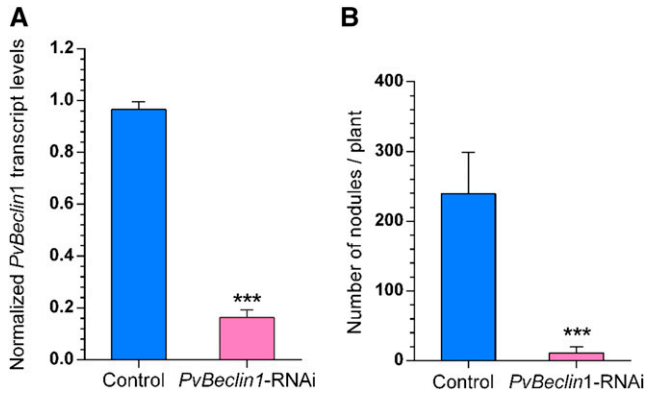

Figure 6. Pv-*Beclin1* Downregulation Impairs Nodulation in *P. vulgaris* Transgenic Roots.

(A) The levels of Pv-*Beclin1* transcript were reduced in transgenic roots expressing *PvBeclin1*-RNAi, compared with control transgenic roots (expressing TdT-*Sac*-RNAi). Transcript levels were normalized using *Elongation Factor 1α* as reference gene, and calculations were made as described in Methods. Bars refer to mean ± SD of four experiments ($n = 4$ from pools of 10 hairy roots). Transcript levels were quantified by RT-qPCR at 14 dpi with *A. rhizogenes* K599. Statistically significant difference is indicated by asterisks (unpaired two-tailed Student's *t* test; ***P < 0.001).

(B) Pv-Beclin1 downregulation led to a decrease in the number of nodules generated at 21 dai with *R. tropici* CIAT 899. Bars are the mean ± SD ($n = 12$ composite plants). Statistically significant differences were confirmed by an unpaired two-tailed Student's *t* test (***P < 0.001).

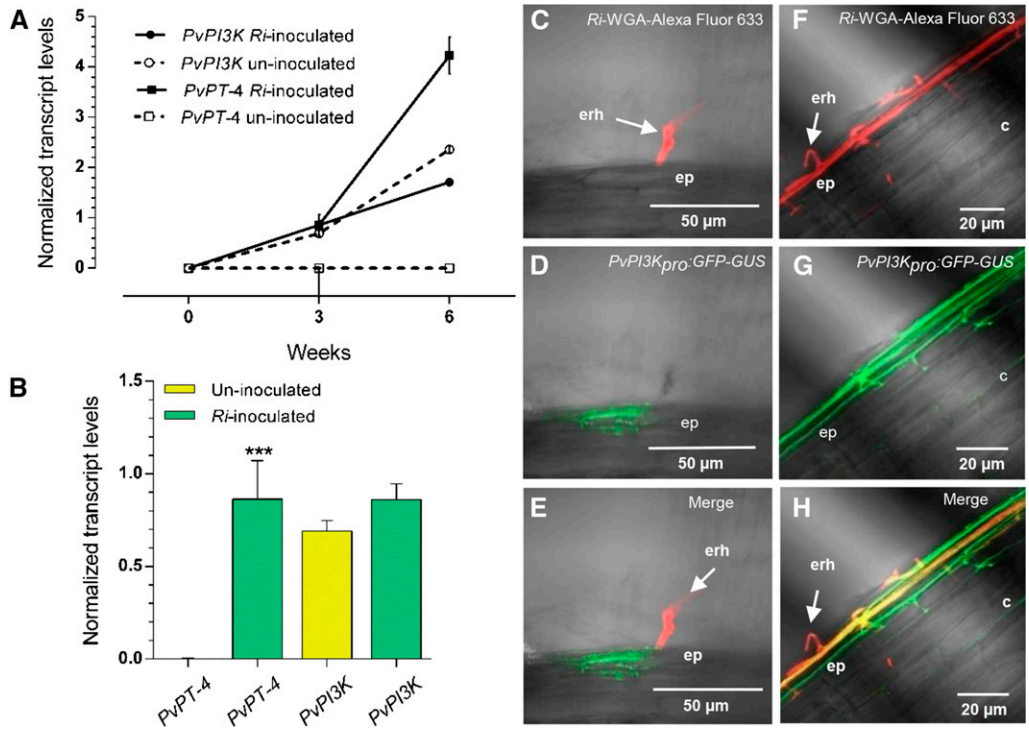

Figure 7. Pv-*PI3K* and Pv-*PT-4* mRNA Levels and Pv-*PI3K* Promoter Activity in *P. vulgaris* Roots after Inoculation with *R. irregularis*.

(A) and **(B)** Pv-*PI3K* and Pv-*PT-4* mRNA levels were quantified by RT-qPCR in wild-type *P. vulgaris* roots inoculated or not with *R. irregularis* and collected at 3 and 6 wai. Transcript levels were normalized to the reference gene *EF1*α, and values were quantified as described in Methods. Normalized Pv-*PT-4* transcript levels are upregulated during the AM symbiosis **(A)**. No significant differences in Pv-*PI3K* transcript level were observed between uninoculated roots and those inoculated with *R. irregularis* **(B)**. Bars indicate mean ± SD from two independent biological replicates ($n = 2$ from a pool of 10 roots). Statistical significance was confirmed by an unpaired two-tailed Student's *t* test (***$P < 0.001$).

(C) to **(H)** *PvPI3K*$_{pro}$*:GFP-GUS* activity, as evaluated by green fluorescence, was detected in epidermal cells neighboring the contact point of the fungal hyphae (**[C]** to **[E]**) and in those beneath the extending extraradical hyphae (**[F]** to **[H]**; merge). AM fungi were stained with WGA-Alexa Fluor 633 conjugate (*Ri*-WGA-Alexa Fluor 633, red fluorescence). Representative images of transgenic roots inoculated with *R. irregularis* and collected at 3 wai. Images were acquired in vivo using a Zeiss LSM 510 Meta Confocal Microscope. ep, epidermis; erh, extraradical hyphae; c, cortex.

shown in Figure 8G, after 3 wai, Pv-*PT-4* transcript levels were lower (0.081 ± 0.009) in Pv-*PI3K* downregulated transgenic roots than in control transgenic roots (0.41 ± 0.036). Together, these results indicate that the AM symbiosis is drastically impaired in Pv-*PI3K* loss-of-function transgenic roots.

DISCUSSION

Leguminous plants, such as common bean, establish mutualistic relationships with soil microorganisms, such as AM fungi, to assimilate phosphate, and with rhizobia, to fix nitrogen symbiotically. In this study, we showed that PI3K has a previously undescribed role in mutualistic interactions. During the *P. vulgaris-Rhizobium* symbiosis, PI3K activity is essential for root hair growth, curling, and IT migration, since these responses were dramatically impaired in Pv-*PI3K* loss-of-function transgenic roots (*PvPI3K*-RNAi hairy roots). These results imply that Pv-PI3K not only plays a key role in supporting polar growth in root hair cells, as has been previously demonstrated (Figure 2F; Lee et al., 2008a), but also during IT growth from cell to cell, since the IT is arrested in the root hair cells and is unable to reach the cortical cells. Surprisingly, cortical cell division was not inhibited in Pv*PI3K*-RNAi hairy roots and nodules developed. However, the few nodules that developed were severely impaired and lacked bacteria, since IT growth and penetration were largely arrested within the root hairs. Since the Pv-*PI3K* promoter is active in the root hair forming the IT and in the dividing cortical cells forming the primordium and thereafter the nodule, we anticipate that Pv-*PI3K* has a distinct role during the infection process and nodule development. This notion is supported by the observation that the few nodules that we did observe were smaller and lacked rhizobia, with some bacteria in the surface at the root hair forming the IT. It is possible that the IT is more sensitive to the absence of PI3P than is cell division, since this latter process was still observed. By the onset of nodule senescence, the Pv-*PI3K* promoter was only active in the nodule vascular bundles, suggesting that Pv-PI3K also functions in nutrient mobilization from the former sink organ.

It is surprising that *R. irregularis* hyphae did not enter the epidermal and cortical cells of Pv*PI3K* loss-of-function bean roots (Pv*PI3K*-RNAi), which resembles the phenotype observed for the rhizobia colonization using the same construction. Consequently,

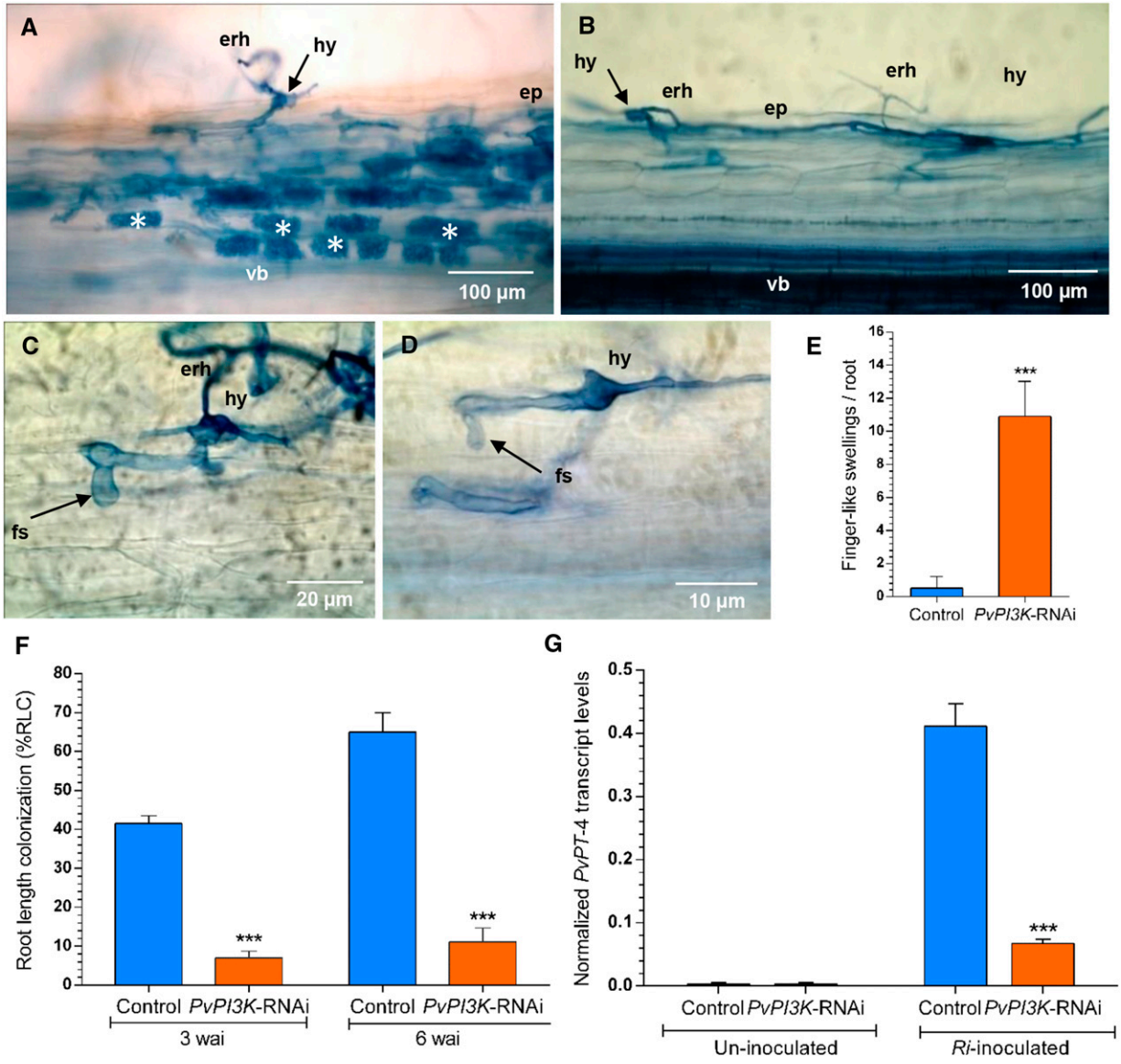

Figure 8. Loss of Function of Pv-*PI3K* Impairs AM Symbiosis in *P. vulgaris* Roots.

(A) to **(D)** AM colonization in PvPI3K-RNAi and control TdT-Sac-RNAi transgenic roots (3 wai) was visualized using trypan blue staining. Bars = 100 µm in **(A)** and **(B)**, 20 µm in **(C)**, and 10 µm in **(D)**.

(A) Control transgenic roots showing typical AM colonization with abundant arbuscules.

(B) PvPI3K-RNAi transgenic roots exhibited sparse hyphae entering and branching inside epidermal cells.

(C) and **(D)** Extraradical hyphae forming branched swellings known as hyphopodia were found. No arbuscules were observed. erh, extraradical hyphae; ep, epidermis; fs, finger-like swelling or outgrowth; hy, hyphopodium; vb, vascular bundle; asterisks, arbuscules.

(E) The number of finger-like outgrowths was higher in PvPI3K-RNAi transgenic roots than in control (TdT-Sac-RNAi) roots inoculated with *R. irregularis* and collected at 3 wai. Data are means ± SD from three independent experiments ($n = 33$). Statistical significance was determined using an unpaired two-tailed Student's *t* test (***$P < 0.001$).

(F) AM colonization was impaired by the loss of function of Pv-PI3K. The root length colonization (%RLC) in PvPI3K-RNAi transgenic roots was lower than in control (TdT-Sac-RNAi) transgenic roots. The data represent means ± SD of three independent experiments ($n = 39$ roots). Statistical significance was determined using an unpaired two-tailed Student's *t* test (***$P < 0.001$).

(G) Transcript level of PvPT-4, the molecular tracker of AM colonization. The expression of PvPT-4 was lower in PvPI3K-RNAi roots inoculated with *R. irregularis* than in inoculated control (TdT-Sac-RNAi) transgenic roots, as determined by RT-qPCR. Transcript levels were normalized to *EF1α* as reference gene. Calculations were made as described in Methods. The bars represent mean ± SD of two experiments ($n = 2$ from a pool of 12 transgenic roots). Asterisks represent statistically significant differences (unpaired two-tailed Student's *t* test, **$P < 0.004$).

typical arbuscules did not form, and tubular protrusions (hyphopodium-like) were observed. These structures were unable to enter epidermal cells. Thus, we have presented compelling data that PI3K plays a key role in both the rhizobial and AM symbiosis in *P. vulgaris* roots. The finding that expressing a domain that specifically binds to PI3P, the catalytic product of PI3K, mimics the loss-of-function phenotype of Pv-*PI3K* in transgenic roots of common bean (Figure 4C), supports the notion that PI3K has a key role in *P. vulgaris* symbiotic interactions.

Root hairs are specialized plant cells, which, like pollen tubes, exhibit highly polarized, tip-localized expansion. Complex signaling networks, involving ion influxes, reactive oxygen species-localized gradients, actin filament reorganization, and enhanced membrane trafficking, operate at the tips of root hair cells (Fu et al., 2001; Hepler et al., 2001; Sieberer et al., 2005; Cárdenas et al., 2008; Oldroyd, 2013). Drugs that inhibit PI3K activity in pollen tubes and root hairs impair proper growth and development (Helling et al., 2006; Lee et al., 2008a, 2008b). The PI3K inhibitors LY294002 and Wortmannin also inhibit the actin filament reorganization induced by abscisic acid in Arabidopsis stomata (Choi et al., 2008). The mechanism by which IT growth is arrested inside root hairs remains unknown, but the mechanism that allows the migration of the IT from one cell to the next seems to be altered in the absence of PI3K. However, we know little about the processes that regulate the passage of the IT from one cell to the next. The nucleus migrates to the base of the root hair to guide IT formation in a cytoskeleton-dependent manner (Lloyd et al., 1897), but how this guidance is regulated is unknown. Our results suggest that PI3K is a key regulator of the polar growth of the IT.

Yeast contains two multiprotein VPS34 complexes that are evolutionarily conserved in autophagy and endocytic sorting. Both of these complexes contain VPS15 and VPS30/ATG6/BECLIN1. One of these complexes also contains ATG14, a regulator of autophagy, and the other contains a second VPS38, which regulates endocytic sorting (Kametaka et al., 1998; Kihara et al., 2001; Kim et al., 2013; Rostislavleva et al., 2015). Interestingly, the complexes are functionally distinct; deletion of *Vps38* inhibits sorting of the lysosomal hydrolase (carboxypeptidase Y) but has no effect on autophagy-induced deprivation, while deletion of *Atg14* and *Atg6*/*Beclin1* inhibits autophagy and does not affect carboxypeptidase Y sorting. Deletion of *Vps34* or *Vps15* results in complete loss of autophagy activity, as described in other mutants defective in autophagy (*aug* mutants) (Tsukada and Ohsumi, 1993; Thumm et al., 1994; Kihara et al., 2001). The main function of the VPS34 complex is to generate PI3P at the phagophore assembly site and recruit PI3P binding proteins. In Arabidopsis, SH3P2 binds to PI3P and ATG8 participates in autophagosome formation (Zhuang et al., 2013). In addition, deletion of *Atg6*/*Beclin1* blocks recruitment of the ATGs required for the phagophore assembly site structure (Suzuki et al., 2001).

In plants, *Vps34*/*PI3K*, *Beclin1*, *Atg3*, and *Atg7* restrict the hypersensitive response-programmed cell death response to tobacco mosaic virus infection (Liu et al., 2005). These findings are consistent with the observation that downregulating Pv-*PI3K* transcript levels with siRNA negatively affected the accumulation of transcripts encoding proteins involved in the formation of the PI3K multiprotein complex and also *Atg8*, which participates in autophagy. Pv-*Beclin1* transcripts were among those that showed reduced accumulation. Fewer nodules formed on the roots of Pv-Beclin1 loss-of-function plants than on those of control plants. We found that Pv-Bec*lin*1 loss-of function in *Pv*PI3K-RNAi hairy roots and overexpression of the FYVE domain in common bean composite plants result in a similar phenotype, suggesting that autophagy is essential for mutualistic interactions between *P. vulgaris* and symbiotic microorganisms.

PI3P levels in plants are relatively low, typically comprising ~2 to 15% of phosphoinositide pools, and they have a rapid turnover rate (Meijer et al., 2001). In Arabidopsis, the role of *PI3K* and PI3P in root hair growth has been examined using PI3K inhibitors or by expressing the 2xFYVE construct under a strong promoter, since homozygous knockout plants (*Vps34* / *Vps34*) are not viable (Gillooly et al., 2000; Vermeer et al., 2006; Lee et al., 2008a). Reducing PI3P levels by expressing the Phosphatase and Tensin homolog deleted on chromosome 10 (PTEN) or by treatment with the WM PI3K inhibitor in tobacco pollen tubes also leads to accumulation of ATG8 in vacuolar autophagic bodies (Zhang et al., 2011). These findings suggest that PI3P levels regulate autophagy genes during the apical growth of root hairs and pollen tubes and that autophagy sustains the rapid growth rate of these cells.

We found that PI3K expression was upregulated 4 d after *R. tropici* inoculation (Figure 1B). However, recently published expression studies suggest that PI3K is not induced during rhizobial infection (Breakspear et al., 2014). The root hair infectome of *M. truncatula* was obtained by monitoring gene expression during rhizobial infection under selected growth conditions. However, no autophagy transcripts were found in the root hair infectome, probably due to the short half-life of autophagy-related transcripts and proteins. Roux et al. (2014) reported that nodule Mt-*PI3K* is highly expressed in the N-fixation zone (Roux et al., 2014), similar to our data, where Pv-*PI3K* transcript levels and *PvPI3K*$_{pro}$*:GFP-GUS* activity also coincided with maximum nitrogen fixation levels in nodules, as depicted in Supplemental Figure 2B.

PI3P binds to proteins through their FYVE domains, which are highly evolutionarily conserved. GFP fusions of these domains have been widely used as probes to monitor the subcellular localization of PI3P (Gillooly et al., 2000; Vermeer et al., 2006). The fact that expressing *YFP*-2xFYVE in bean hairy roots phenocopies the loss of function of Pv-*PI3K* strongly suggests that PI3P, the catalytic product of PI3K, is essential for the mutualistic interactions of *P. vulgaris* with AM fungi and rhizobia.

Our results suggest that autophagy provides precursors for root hair and IT growth, but apparently not for cortical cell divisions during common bean nodule organogenesis. The root epidermis penetration sites by hyphae (hyphopodia) and arbuscule formation of AM fungi also appear to require precursors derived from the autophagic process. Recently, Mi et al. (2015) reported that actin polymerization into short filaments and PI3P levels are crucial for both processes, since the shape and expansion of phagophores (the precursors of autophagosomes) depend on both of these processes to initiate autophagy, indicating that actin polymerization is regulated by the omegasome (i.e., the endoplasmic reticulum membrane protrusion enriched in the PI3P pool; Mi et al., 2015). This indicates that actin functions during the early stages of autophagosome formation. Specifically, dynamic actin polymerization and branching form a three-dimensional structure that supports the assembly of the omegasome and isolation

membrane. Together, these data indicate that autophagy is a key player in mutualistic interactions between plants and symbiotic microorganisms.

METHODS

Bean Hairy Root Transformation

Common bean seeds (*Phaseolus vulgaris* cv Negro Jamapa) were used for *Agrobacterium rhizogenes* K599-mediated transformation to generate hairy roots in composite plants using a previously described method (Estrada-Navarrete et al., 2007). Usually at the second week after inoculation, hairy roots emerging from *A. rhizogenes* K599-induced calli are ~3 cm long. When indicated, hairy roots were observed under an epifluorescence stereomicroscope (Olympus SZX7) and red fluorescent transgenic roots were selected on the basis of the expression of red fluorescent protein tdTomato (tandem dimer Tomato; Shaner et al., 2004) encoded by pTDT-DC-RNAi-derived constructs. Nonfluorescent hairy roots were excised with a scalpel from the site of emergence and discarded. Hairy roots were either frozen in liquid nitrogen and stored at −80°C or subjected to phenotype analysis.

Identification of the *PI3K* Gene in *P. vulgaris*

To identify *P. vulgaris* genomic sequences encoding a PI3K ortholog, the oligonucleotides PI3K_F and PI3K_R (Supplemental Table 1), based on the *Glycine max* PI3K cDNA sequence (Hong and Verma, 1994), were used in an RT-PCR reaction containing RNA extracted from common bean nodules (at 20 dai). The amplified fragment (847 bp) was further used as a probe to screen *P. vulgaris* genomic and cDNA libraries. A BLASTX sequence analysis of the isolated cDNA (2793 bp) and genomic clones (13.07 kb) isolated showed that both contain an open reading frame of 2436 bp encoding the same protein sequence (811 amino acids), which was 84% identical to *Arabidopsis thaliana* VPS34 (PI3K). The sequence of Pv-*PI3K*, originally reported in the GenBank database under accession number DQ118424.2, is identical to the sequence with ID number Phvul.002G070100.1 available in the Phytozome v11 database (http://www.phytozome.net).

Vector Construction

To generate the *PvPI3K*$_{pro}$*:GFP-GUS* construct, a 1050-bp fragment upstream of the Pv-*PI3K* initiation codon was amplified by PCR using *P. vulgaris* cv Negro Jamapa genomic DNA as template and the gene-specific primers *PvPI3K*$_{pro}$–F and *PvPI3K*$_{pro}$–R (Supplemental Table 1). The PCR product was cloned into the pENTR/D-TOPO vector (Invitrogen), confirmed by sequencing, and recombined into the destination binary vector pBGWFS7,0 (Karimi et al., 2002) using Gateway LR Clonase II Enzyme Mix (Invitrogen). To create the *PvPI3K*-RNAi construct, a 537-bp fragment corresponding to the 3′-coding region of Pv-*PI3K* was amplified by PCR using the primers *PvPI3K*-RNAi_F and *PvPI3K*-RNAi_R (Supplemental Table 1) and cDNA from *P. vulgaris* nodules (20 dai). After cloning this fragment into pENTR/D-TOPO (Invitrogen) and confirming the presence of the insert by sequencing, the PCR product was recombined into the compatible recombination sites of the Gateway-based hairpin pTDT-DC-RNAi vector (Valdés-López et al., 2008). The correct orientation of the recombined fragments was confirmed by sequencing and by PCR using the primers Wrky-3_F or Wrky-5_R with *PvPI3K*-RNAi_F (Supplemental Table 1), as described (Valdés-López et al., 2008). The resulting construct (pTDT-*PvPI3K*-RNAi) drives the transcription of a hairpin loop *PvPI3K*-RNAi under control of the 35S promoter. The pTDT-DC-RNAi vector also harbors the *NOS*$_{pro}$*:tdT* cassette, which mediates the hairy root expression of the molecular fluorescent marker tdTomato (Shaner et al., 2004) and allows identification of transformed roots. The *PvBeclin1*-RNAi construct was generated by recombining a Pv-*Beclin1* fragment (400 bp of 5′-untranslated region) amplified by PCR using the primers *PvBeclin1*-RNAi_F and *PvBeclin1*_RNAi_R (Supplemental Table 1). To overexpress the FYVE domain, the pGreen35S:YFP-2xFYVE plasmid, kindly provided by Teun Munnik (Vermeer et al., 2006), was used. All constructed plasmids were introduced by electroporation into *A. rhizogenes* strain K599.

Nodulation Assays

Rhizobium tropici CIAT899 bacteria were grown in 250-mL flasks containing 100 mL of PY broth supplemented with 7 mM $CaCl_2$, 50 μg/mL rifampicin, and 20 μg/mL nalidixic acid, in a shaking incubator (250 rpm) at 30°C until the suspension reached an OD_{600} of 0.8. For nodulation assays, transgenic composite plants were transplanted to pots (10 × 10 cm) containing sterile vermiculite, inoculated with 1 mL of a suspension of *R. tropici* CIAT899 diluted to an OD_{600} of 0.05 in 10 mM $MgSO_4$, and grown in a controlled environmental chamber (16 h light/8 h darkness, at 26°C). Plants were watered three to four times per week with Broughton and Dilworth (B&D; Broughton and Dilworth, 1971) solution containing 2 mM KNO_3. At the indicated time points after inoculation, transgenic roots were frozen in liquid nitrogen and stored at −80°C or analyzed to detect a phenotype.

Quantification of Transcript Levels by RT-qPCR Analysis

Total RNA was extracted from frozen tissues using TRIzol reagent (Life Technologies) following the manufacturer's instructions. To eliminate contaminating genomic DNA, total RNA samples (1 μg in 20 μL) were treated with 1 unit of DNaseI (RNase-free; Invitrogen) at 37°C for 30 min and then at 65°C for 10 min. Two-step RT-qPCR was performed using a Maxima First Strand cDNA Synthesis Kit for RT-qPCR (ThermoFisher Scientific) and Maxima SYBR Green qPCR Master Mix (2X; ThermoFisher Scientific), respectively, following the manufacturer's instructions. Each reaction was set up using 100 ng of cDNA as template in a 20 μL final volume. Gene-specific primers used in RT-qPCR reactions are listed in Supplemental Table 1. qPCRs were performed in a LightCycler 480 real-time PCR system (Roche). Relative transcript abundance was calculated using one the following formulae (Schmittgen and Livak, 2008):

$$2^{-\Delta C_T} = [(C_T \text{ gene of interest} - C_T \text{ reference gene})]$$

or

$$2^{-\Delta\Delta C_T} = [(C_T \text{ gene of interest} - C_T \text{ reference gene}) \text{ sample A} - (C_T \text{ gene of interest} - C_T \text{ reference gene}) \text{ sample B})]$$

*P. vulgaris Elongation Factor 1*α (Pv-*EF1*α) was used as a reference gene, as previously described. RT-qPCR data are averages of three or four independent experiments or biological replicates, and each sample was assessed in triplicate.

Root Hair and Root Tip Isolation

Root hairs were isolated according to a protocol posted on the Root Hair Systems Biology website at Gary Stacey Laboratory, University of Missouri-Columbia, MO (http://www.soyroothair.org/index.php/education/4-research/protocols/12-root-hair-isolation-protocol). Briefly, *P. vulgaris* seedlings (48 h after germination) were held with tweezers and the root tips (~0.5 mm) were cut from the seedlings with scissors. A second cut, at the base of the root, released the remaining segment of root. The freshly harvested root tips and root segments were dropped into separate beakers containing liquid nitrogen and stirred vigorously to separate the root hairs from the roots. Root hairs were isolated by pouring the liquid nitrogen

mixture through a metal strainer. After nitrogen evaporation, root hairs, root tips, and stripped roots (which were retained in the strainer) were collected and stored at −80°C as separate frozen fractions until use.

Mycorrhizal Spore Inoculation and Mycorrhization

Composite bean plants (*PvPI3K*-RNAi and control) were transferred into pots (20-cm diameter) with sterile Metro-Mix and inoculated with 800 spores of *Rhizophagus irregularis* (kindly provided by Ignacio M. Mendoza, Instituto Politécnico Nacional, Mexico) per plant. Inoculated plants were irrigated twice weekly with half-strength B&D solution containing a low concentration of potassium phosphate (10 μM) to favor AM colonization (Smith et al., 2003). Infected roots were collected from plants at 21 and 42 dai, and AM fungi were stained either with Trypan blue (according to a modified staining procedure in Koske and Gemma, 1989) or with WGA conjugated to Alexa Fluor 633 (WGA-Alexa Fluor 633; Molecular Probes) as described before (Javot et al., 2007). AM fungal colonization status was determined by light and confocal microscopy, as indicated. The %RLC, including all fungal structures, was estimated by the magnified intersection method described by McGonigle et al. (1990).

Microscopy and Image Analysis

Transgenic roots were cleared and mounted in a solution containing 4.2 M NaI and 8 mM $Na_2S_2O_3$ in 65% glycerol and 2% DMSO, as described (Dubrovsky et al., 2009). Prior to observation, root sections of ~3 cm in length were mounted in rows on a glass microscope slide. The number of root hairs having a length of >130 or <130 μm per millimeter of mounted root was determined based on images captured using a NA40 ×/1 water immersion objective lens on a Zeiss Axiovert 200M microscope equipped with Nomarski optics and coupled to a Photometrics CoolSNAPcf Color Camera (Valley International). ITs and hand-sectioned nodules were analyzed in transgenic roots collected at 12 to 17 dai and observed under a confocal microscope. To visualize AM fungal structures, the roots were stained with Trypan blue and observed using a Zeiss Axioskop microscope with 10×, 20×, and 63× lenses. Infected roots were stained with WGA conjugated to Alexa Fluor 633 and observed under a confocal microscope. Transgenic roots harboring *PvPI3K$_{pro}$:GFP-GUS* were subjected to histochemical analysis of GUS activity, as described previously (Jefferson et al., 1987). Sample transgenic roots were observed under a Zeiss Axioskop microscope using 10×, 20×, and 63× lenses or by confocal microscopy. When indicated, the confocal microscopy analysis was performed at the Laboratorio Nacional de Microscopía Avanzada (LNMA-IBT UNAM) facility, using a Zeiss LSM 510 Meta Confocal Microscope. GFP fluorescence was excited with an argon/2 ion laser (488 nm), and emitted fluorescence was collected using a band-pass 500- to 530-nm IR filter. TdT and DsRed fluorescence were excited at 543 nm by a laser, and emission was filtered using a long-pass 560-nm filter. WGA-Alexa Fluor 633 (red channel) was excited by a HeNe2 laser at 633 nm, and the emitted fluorescence was collected using a band-pass 507-IR filter.

Acetylene Reduction

Nitrogen fixation was assessed using the acetylene reduction method (Vessey, 1994). Transgenic nodulated roots (20 dai; six individual roots per experiment) were placed in a 160-mL vial closed with a serum cap. Air (2 mL) was immediately withdrawn from the closed vial and replaced with an equal volume of acetylene gas. Samples were incubated for 60 min at room temperature, and ethylene production was assayed by gas chromatography in a Variant model 3300 chromatograph. Immediately after gas chromatography, nodules were separated from the roots and allowed to dry at 60°C for 2 d. Specific activity is expressed as mmol of ethylene/h/g of nodule dry weight.

Phylogenetic Analysis

Amino acid sequences of PI3K class III proteins were retrieved from GenBank (http://www.ncbi.nlm.nih.gov/genbank/), EMBL-EBI (http://www.ebi.ac.uk/), Phytozome c11 (http://www.phytozome.net), and PLAZA (http://bioinformatics.psb.ugent.be/plaza/). Multiple sequence alignment was performed using the ClustalW algorithm, and the phylogenetic tree was generated using the neighbor-joining method with 1000 bootstrap trials, and both procedures were implemented in MEGA7 (Thompson et al., 1997). The phylogenetic tree was generated using MEGA7 (http://www.megasoftware.net/; Tamura et al., 2011).

Statistical Analysis

Data processing and statistical analysis were performed using GraphPad Prism version 6.00 for Windows (GraphPad Software). An unpaired two-tailed Student's *t* test was used to determine whether data from two different groups were statistically significantly different or one-way ANOVA was performed for multiple comparisons. Single, double, and triple asterisks above the columns indicate differences that are statistically significant ($P < 0.05$ or $P < 0.01$) or very significant ($P < 0.001$), respectively.

Accession Numbers

Sequence data from this article can be found in the GenBank/EMBL databases under the following accession numbers for PI3K class III proteins: *Glycine max* root isoform (NP_001236955.1), *G. max* nodule isoform (NP_001242315.1), *P. vulgaris* (ABA03136.1), *Medicago truncatula* (CAD56881.1), *Populus trichocarpa* (XP002318628.1), *Vitis vinifera* root isoform (XP_002267769.2), *Nicotiana tabacum* (AAW80628.1), *Solanum lycopersicum* (XP_004236633.1), *Arabidopsis thaliana* (AEE33693.1; AT1G60490.1), *Brassica napus* (AAN62481.1), *Physcomitrella patens* (XP_001762959.1), *Zea mays* (AFW62054.1), *Hordeum vulgare* (BAJ91813.1), *Triticum urartu* (EMS55477), *Oryza sativa* japonica 2 (NP_001054810.1), *O. sativa* japonica 1 (NP_001061506.1), *Amborella trichopoda* (ERN10666.1), *Micromonas* sp (XP_002506109.1), *Chlamydomonas reinhardtii* (XP_001689631.1), *Dictyostelium discoideum* (AAA85726.1), *Saccharomyces cerevisiae* (EDV08569.1), *Candida albicans* (Q92213), *Schizosaccharomyces pombe* (AAC49133.1), *Trametes versicolor* (EIW57772.1), *Talaromyces marneffei* (XP_002147483.1), *Aspergillus oryzae* (XP_001824747.1), *Neosartorya fischeri* (XP_001259818.1), *Drosophila melanogaster* (NP_477133.1), *Homo sapiens* (NP_002638.2), and *Mus musculus* (AAH24675.1).

Supplemental Data

Supplemental Figure 1. Phylogenetic tree of *PI3K* class III proteins.

Supplemental Figure 2. Pv-*PI3K* transcript levels during nodule development and tissue-specific activity of the Pv-*PI3K* promoter in mature and senescent nodules.

Supplemental Figure 3. Quantification of Pv-*PI3K* transcript levels in individual *PvPI3K*-RNAi transgenic roots.

Supplemental Figure 4. Loss of function of Pv-*PI3K* led to a reduction of *Phaseolus vulgaris* nodule number and impaired root nodule development.

Supplemental Figure 5. Extraradical hyphae growth and finger-like swellings are increased after *Rhizophagus irregularis* inoculation in *PvPI3K* loss of function of *P. vulgaris* roots.

Supplemental Table 1. Oligonucleotides used in this study.

Supplemental Table 2. Quantification of root hairs and curling in loss of function of *PvPI3K* and control *P. vulgaris* roots.

Supplemental Data Set 1. Text file of the alignment used to generate the phylogenetic tree of PI3K class III proteins shown in Supplemental Figure 1.

ACKNOWLEDGMENTS

We thank Rosana Sánchez for her valuable contribution to the manuscript edition in its final version. We also thank members of F.S.'s laboratory for their helpful comments and discussions. We thank Teun Munnik (Section of Plant Physiology, Swammerdam Institute for Life Sciences, University of Amsterdam, Amsterdam, The Netherlands) for providing the vector pGreen35S:YFP-2xFYVE. We thank Nelson Avonce for help and support with the phylogenetic analysis. We thank Olivia Santana, Chandrasekar B. Rajeswari, Carlos A. González Chávez, and Noreide Nava (Instituto de Biotecnología, Universidad Nacional Autónoma de México [UNAM]) for technical support. We thank Eugenio López and Arturo Yañez (Instituto de Biotecnología, UNAM) for synthesis of oligonucleotides. We thank Guillermo Krotzsch (Instituto de Física, UNAM) for helpful support with the images and figures. We thank Alfonso Leija for technical support with the acetylene assays (CCG-UNAM). This study was funded by CONACYT 177744 and DGAPA-IN206415.

AUTHOR CONTRIBUTIONS

F.S., G.E.-N., and R.L. conceived the study. F.S., G.E.-N., C.Q., and M.-K.A. designed the experiments. G.E.-N., N.C.-M., and R.L. produced the vector constructs. A.H.-B., L.C., J.E.O., and G.E.-N. performed quantitative analysis of root hairs. M.-K.A. and G.E.-N. performed phenotypic analyses of mycorrhizal transgenic roots. F.S., X.A.-A., G.E.-N., and N.C.-M. performed the confocal microscopy image analysis. G.E.-N., N.C.-M., and A.B. analyzed the experimental data, produced the graphs, and conducted the RT-qPCR analysis. F.S., L.C., C.Q., and G.E.-N. wrote the article.

Received December 10, 2015; revised July 18, 2016; accepted August 29, 2016; published August 30, 2016.

REFERENCES

Arthikala, M.K., Montiel, J., Nava, N., Santana, O., Sánchez-López, R., Cárdenas, L., and Quinto, C. (2013). PvRbohB negatively regulates *Rhizophagus irregularis* colonization in *Phaseolus vulgaris.* Plant Cell Physiol. **54:** 1391–1402.

Blanco, F.A., Meschini, E.P., Zanetti, M.E., and Aguilar, O.M. (2009). A small GTPase of the Rab family is required for root hair formation and preinfection stages of the common bean-Rhizobium symbiotic association. Plant Cell **21:** 2797–2810.

Bonfante, P., and Genre, A. (2008). Plants and arbuscular mycorrhizal fungi: an evolutionary-developmental perspective. Trends Plant Sci. **13:** 492–498.

Breakspear, A., Liu, C., Roy, S., Stacey, N., Rogers, C., Trick, M., Morieri, G., Mysore, K.S., Wen, J., Oldroyd, G.E., Downie, J.A., and Murray, J.D. (2014). The root hair "infectome" of *Medicago truncatula* uncovers changes in cell cycle genes and reveals a requirement for Auxin signaling in rhizobial infection. Plant Cell **26:** 4680–4701.

Brearley, C.A., and Hanke, D.E. (1992). 3- and 4-Phosphorylated phosphatidylinositols in the aquatic plant *Spirodela polyrhiza* L. Biochem. J. **283:** 255–260.

Broughton, W.J., and Dilworth, M. (1971). Control of leghaemoglobin synthesis in snake beans. Biochem. J. **125:** 1075–1080.

Cárdenas, L., Lovy-Wheeler, A., Kunkel, J.G., and Hepler, P.K. (2008). Pollen tube growth oscillations and intracellular calcium levels are reversibly modulated by actin polymerization. Plant Physiol. **146:** 1611–1621.

Cárdenas, L., Holdaway-Clarke, T.L., Sánchez, F., Quinto, C., Feijo, J.A., Kunkel, J.G., and Hepler, P.K. (2000). Ion changes in legume root hairs responding to Nod factors. Plant Physiol. **123:** 443–452.

Crespi, M.D., Jurkevitch, E., Poiret, M., d'Aubenton-Carafa, Y., Petrovics, G., Kondorosi, E., and Kondorosi, A. (1994). *enod40*, a gene expressed during nodule organogenesis, codes for a non-translatable RNA involved in plant growth. EMBO J. **13:** 5099–5112.

Charron, D., Pingret, J.L., Chabaud, M., Journet, E.P., and Barker, D.G. (2004). Pharmacological evidence that multiple phospholipid signaling pathways link Rhizobium nodulation factor perception in *Medicago truncatula* root hairs to intracellular responses, including Ca^{2+} spiking and specific ENOD gene expression. Plant Physiol. **136:** 3582–3593.

Choi, Y., Lee, Y., Jeon, B.W., Staiger, C.J., and Lee, Y. (2008). Phosphatidylinositol 3- and 4-phosphate modulate actin filament reorganization in guard cells of day flower. Plant Cell Environ. **31:** 366–377.

Dolan, L., Janmaat, K., Willemsen, V., Linstead, P., Poethig, S., Roberts, K., and Scheres, B. (1993). Cellular organisation of the *Arabidopsis thaliana* root. Development **119:** 71–84.

Dubrovsky, J.G., Soukup, A., Napsucialy-Mendivil, S., Jeknic, Z., and Ivanchenko, M.G. (2009). The lateral root initiation index: an integrative measure of primordium formation. Ann. Bot. (Lond.) **103:** 807–817.

Engstrom, E.M., Ehrhardt, D.W., Mitra, R.M., and Long, S.R. (2002). Pharmacological analysis of nod factor-induced calcium spiking in *Medicago truncatula*. Evidence for the requirement of type IIA calcium pumps and phosphoinositide signaling. Plant Physiol. **128:** 1390–1401.

Estrada-Navarrete, G., Alvarado-Affantranger, X., Olivares, J.E., Guillén, G., Díaz-Camino, C., Campos, F., Quinto, C., Gresshoff, P.M., and Sánchez, F. (2007). Fast, efficient and reproducible genetic transformation of Phaseolus spp. by *Agrobacterium rhizogenes.* Nat. Protoc. **2:** 1819–1824.

Fu, Y., Wu, G., and Yang, Z. (2001). Rop GTPase-dependent dynamics of tip-localized F-actin controls tip growth in pollen tubes. J. Cell Biol. **152:** 1019–1032.

Gaullier, J.M., Simonsen, A., D'Arrigo, A., Bremnes, B., Stenmark, H., and Aasland, R. (1998). FYVE fingers bind PtdIns(3)P. Nature **394:** 432–433.

Genre, A., Chabaud, M., Faccio, A., Barker, D.G., and Bonfante, P. (2008). Prepenetration apparatus assembly precedes and predicts the colonization patterns of arbuscular mycorrhizal fungi within the root cortex of both *Medicago truncatul*a and *Daucus carota.* Plant Cell **20:** 1407–1420.

Gillooly, D.J., Morrow, I.C., Lindsay, M., Gould, R., Bryant, N.J., Gaullier, J.M., Parton, R.G., and Stenmark, H. (2000). Localization of phosphatidylinositol 3-phosphate in yeast and mammalian cells. EMBO J. **19:** 4577–4588.

Hanaoka, H., Noda, T., Shirano, Y., Kato, T., Hayashi, H., Shibata, D., Tabata, S., and Ohsumi, Y. (2002). Leaf senescence and starvation-induced chlorosis are accelerated by the disruption of an Arabidopsis autophagy gene. Plant Physiol. **129:** 1181–1193.

Helling, D., Possart, A., Cottier, S., Klahre, U., and Kost, B. (2006). Pollen tube tip growth depends on plasma membrane polarization mediated by tobacco PLC3 activity and endocytic membrane recycling. Plant Cell **18:** 3519–3534.

Hepler, P.K., Vidali, L., and Cheung, A.Y. (2001). Polarized cell growth in higher plants. Annu. Rev. Cell Dev. Biol. **17:** 159–187.

Herman, P.K., and Emr, S.D. (1990). Characterization of VPS34, a gene required for vacuolar protein sorting and vacuole segregation in *Saccharomyces cerevisiae.* Mol. Cell. Biol. **10:** 6742–6754.

Hiles, I.D., et al. (1992). Phosphatidylinositol 3-kinase: structure and expression of the 110 kd catalytic subunit. Cell **70:** 419–429.

Hong, Z., and Verma, D.P. (1994). A phosphatidylinositol 3-kinase is induced during soybean nodule organogenesis and is associated with membrane proliferation. Proc. Natl. Acad. Sci. USA **91:** 9617–9621.

Javot, H., Penmetsa, R.V., Terzaghi, N., Cook, D.R., and Harrison, M.J. (2007). A *Medicago truncatula* phosphate transporter indispensable for the arbuscular mycorrhizal symbiosis. Proc. Natl. Acad. Sci. USA **104:** 1720–1725.

Jefferson, R.A., Kavanagh, T.A., and Bevan, M.W. (1987). GUS fusions: b-glucuronidase as a sensitive and versatile gene fusion marker in higher plants. EMBO J. **6:** 3901–3907.

Kale, S.D., et al. (2010). External lipid PI3P mediates entry of eukaryotic pathogen effectors into plant and animal host cells. Cell **142:** 284–295.

Kametaka, S., Okano, T., Ohsumi, M., and Ohsumi, Y. (1998). Apg14p and Apg6/Vps30p form a protein complex essential for autophagy in the yeast, *Saccharomyces cerevisiae.* J. Biol. Chem. **273:** 22284–22291.

Karimi, M., Inze, D., and Depicker, A. (2002). GATEWAY vectors for Agrobacterium-mediated plant transformation. Trends Plant Sci. **7:** 193–195.

Kihara, A., Kabeya, Y., Ohsumi, Y., and Yoshimori, T. (2001). Beclin-phosphatidylinositol 3-kinase complex functions at the trans-Golgi network. EMBO Rep. **2:** 330–335.

Kim, J., Kim, Y.C., Fang, C., Russell, R.C., Kim, J.H., Fan, W., Liu, R., Zhong, Q., and Guan, K.L. (2013). Differential regulation of distinct Vps34 complexes by AMPK in nutrient stress and autophagy. Cell **152:** 290–303.

Klionsky, D.J., and Ohsumi, Y. (1999). Vacuolar import of proteins and organelles from the cytoplasm. Annu. Rev. Cell Dev. Biol. **15:** 1–32.

Koske, R.E., and Gemma, J.N. (1989). A modified procedure for staining roots to detect V-A mycorrhizas. Mycol. Res. **92:** 486–488.

Kumagai, H., Kinoshita, E., Ridge, R.W., and Kouchi, H. (2006). RNAi knock-down of ENOD40s leads to significant suppression of nodule formation in *Lotus japonicus.* Plant Cell Physiol. **47:** 1102–1111.

Lee, Y., Bak, G., Choi, Y., Chuang, W.I., Cho, H.T., and Lee, Y. (2008a). Roles of phosphatidylinositol 3-kinase in root hair growth. Plant Physiol. **147:** 624–635.

Lee, Y., Kim, E.S., Choi, Y., Hwang, I., Staiger, C.J., Chung, Y.Y., and Lee, Y. (2008b). The Arabidopsis phosphatidylinositol 3-kinase is important for pollen development. Plant Physiol. **147:** 1886–1897.

Levine, B., and Klionsky, D.J. (2004). Development by self-digestion: molecular mechanisms and biological functions of autophagy. Dev. Cell **6:** 463–477.

Liu, Y., Schiff, M., Czymmek, K., Talloczy, Z., Levine, B., and Dinesh-Kumar, S.P. (2005). Autophagy regulates programmed cell death during the plant innate immune response. Cell **121:** 567–577.

Lloyd, C.W., Pearce, K.J., Rawlins, D.J., Ridge, R.W., and Shaw, P.J. (1897). Endoplasmic microtubules connect the advancing nucleus to the tip of legume root hairs, but F-actin is involved in basipetal migration. Cell Motil. Cytoskeleton **8:** 27–36.

McGonigle, T.P., Millers, M.H., Evans, D.G., Fairchild, G.L., and Swan, J.A. (1990). A new method which gives an objective measure of colonization of roots by vesicular-arbuscular mycorrhizal fungi. New Phytol. **115:** 495–501.

Meijer, H.J., Berrie, C.P., Iurisci, C., Divecha, N., Musgrave, A., and Munnik, T. (2001). Identification of a new polyphosphoinositide in plants, phosphatidylinositol 5-monophosphate (PtdIns5P), and its accumulation upon osmotic stress. Biochem. J. **360:** 491–498.

Mi, N., et al. (2015). CapZ regulates autophagosomal membrane shaping by promoting actin assembly inside the isolation membrane. Nat. Cell Biol. **17:** 1112–1123.

Montiel, J., Nava, N., Cardenas, L., Sanchez-Lopez, R., Arthikala, M.K., Santana, O., Sanchez, F., and Quinto, C. (2012). A *Phaseolus vulgaris* NADPH oxidase gene is required for root infection by Rhizobia. Plant Cell Physiol. **53:** 1751–1767.

Mylona, P., Pawlowski, K., and Bisseling, T. (1995). Symbiotic nitrogen fixation. Plant Cell **7:** 869–885.

Okazaki, S., Kaneko, T., Sato, S., and Saeki, K. (2013). Hijacking of leguminous nodulation signaling by the rhizobial type III secretion system. Proc. Natl. Acad. Sci. USA **110:** 17131–17136.

Oldroyd, G.E. (2013). Speak, friend, and enter: signalling systems that promote beneficial symbiotic associations in plants. Nat. Rev. Microbiol.**11:** 252–263.

Oldroyd, G.E., and Downie, J.A. (2008). Coordinating nodule morphogenesis with rhizobial infection in legumes. Annu. Rev. Plant Biol. **59:** 519–546.

Parniske, M. (2008). Arbuscular mycorrhiza: the mother of plant root endosymbioses. Nat. Rev. Microbiol. **6:** 763–775.

Patki, V., Lawe, D.C., Corvera, S., Virbasius, J.V., and Chawla, A. (1998). A functional PtdIns(3)P-binding motif. Nature **394:** 433–434.

Peleg-Grossman, S., Volpin, H., and Levine, A. (2007). Root hair curling and Rhizobium infection in *Medicago truncatula* are mediated by phosphatidylinositide-regulated endocytosis and reactive oxygen species. J. Exp. Bot. **58:** 1637–1649.

Pingret, J.L., Journet, E.P., and Barker, D.G. (1998). Rhizobium nod factor signaling. Evidence for a g protein-mediated transduction mechanism. Plant Cell **10:** 659–672.

Qin, G., Ma, Z., Zhang, L., Xing, S., Hou, X., Deng, J., Liu, J., Chen, Z., Qu, L.J., and Gu, H. (2007). Arabidopsis AtBECLIN 1/AtAtg6/AtVps30 is essential for pollen germination and plant development. Cell Res. **17:** 249–263.

Rostislavleva, K., Soler, N., Ohashi, Y., Zhang, L., Pardon, E., Burke, J.E., Masson, G.R., Johnson, C., Steyaert, J., Ktistakis, N.T., and Williams, R.L. (2015). Structure and flexibility of the endosomal Vps34 complex reveals the basis of its function on membranes. Science **350:** aac7365.

Roux, B., et al. (2014). An integrated analysis of plant and bacterial gene expression in symbiotic root nodules using laser-capture microdissection coupled to RNA sequencing. Plant J. **77:** 817–837.

Schmittgen, T.D., and Livak, K.J. (2008). Analyzing real-time PCR data by the comparative C(T) method. Nat. Protoc. **3:** 1101–1108.

Shaner, N.C., Campbell, R.E., Steinbach, P.A., Giepmans, B.N., Palmer, A.E., and Tsien, R.Y. (2004). Improved monomeric red, orange and yellow fluorescent proteins derived from Discosoma sp. red fluorescent protein. Nat. Biotechnol. **22:** 1567–1572.

Sieberer, B.J., Ketelaar, T., Esseling, J.J., and Emons, A.M. (2005). Microtubules guide root hair tip growth. New Phytol. **167:** 711–719.

Smith, S.E., Smith, F.A., and Jakobsen, I. (2003). Mycorrhizal fungi can dominate phosphate supply to plants irrespective of growth responses. Plant Physiol. **133:** 16–20.

Stack, J.H., and Emr, S.D. (1993). Genetic and biochemical studies of protein sorting to the yeast vacuole. Curr. Opin. Cell Biol. **5:** 641–646.

Stack, J.H., DeWald, D.B., Takegawa, K., and Emr, S.D. (1995). Vesicle-mediated protein transport: regulatory interactions between the Vps15 protein kinase and the Vps34 PtdIns 3-kinase essential for protein sorting to the vacuole in yeast. J. Cell Biol. **129:** 321–334.

Stenmark, H., Aasland, R., Toh, B.H., and D'Arrigo, A. (1996). Endosomal localization of the autoantigen EEA1 is mediated by a zinc-binding FYVE finger. J. Biol. Chem. **271:** 24048–24054.

Suzuki, K., Kirisako, T., Kamada, Y., Mizushima, N., Noda, T., and Ohsumi, Y. (2001). The pre-autophagosomal structure organized by concerted functions of APG genes is essential for autophagosome formation. EMBO J. **20:** 5971–5981.

Tamura, K., Peterson, D., Peterson, N., Stecher, G., Nei, M., and Kumar, S. (2011). MEGA5: Molecular evolutionary genetics analysis using likelihood, distance, and parsimony methods. Mol. Biol. Evol. **28:** 2731–2739.

Thompson, A.R., and Vierstra, R.D. (2005). Autophagic recycling: lessons from yeast help define the process in plants. Curr. Opin. Plant Biol. **8:** 165–173.

Thompson, J.D., Gibson, T.J., Plewniak, F., Jeanmougin, F., and Higgins, D.G. (1997). The CLUSTAL_X windows interface: flexible strategies for multiple sequence alignment aided by quality analysis tools. Nucleic Acids Res. **25:** 4876–4882.

Thumm, M., Egner, R., Koch, B., Schlumpberger, M., Straub, M., Veenhuis, M., and Wolf, D.H. (1994). Isolation of autophagocytosis mutants of *Saccharomyces cerevisiae.* FEBS Lett. **349:** 275–280.

Tsukada, M., and Ohsumi, Y. (1993). Isolation and characterization of autophagy-defective mutants of Saccharomyces cerevisiae. FEBS Lett. **333:** 169–174.

Valdés-López, O., Arenas-Huertero, C., Ramírez, M., Girard, L., Sanchez, F., Vance, C.P., Luis Reyes, J., and Hernández, G. (2008). Essential role of MYB transcription factor: PvPHR1 and microRNA: PvmiR399 in phosphorus-deficiency signalling in common bean roots. Plant Cell Environ. **31:** 1834–1843.

Vanhaesebroeck, B., Guillermet-Guibert, J., Graupera, M., and Bilanges, B. (2010). The emerging mechanisms of isoform-specific PI3K signalling. Nat. Rev. Mol. Cell Biol. **11:** 329–341.

van Spronsen, P.C., Gronlund, M., Pacios Bras, C., Spaink, H.P., and Kijne, J.W. (2001). Cell biological changes of outer cortical root cells in early determinate nodulation. Mol. Plant Microbe Interact. **14:** 839–847.

Vermeer, J.E., van Leeuwen, W., Tobena-Santamaria, R., Laxalt, A.M., Jones, D.R., Divecha, N., Gadella, T.W., Jr., and Munnik, T. (2006). Visualization of PtdIns3P dynamics in living plant cells. Plant J. **47:** 687–700.

Vessey, J.K. (1994). Measurement of nitrogenase activity in legume root nodules: in defence of the acetylene reduction assay. Plant Soil **158:** 151–162.

Walker, E.H., Perisic, O., Ried, C., Stephens, L., and Williams, R.L. (1999). Structural insights into phosphoinositide 3-kinase catalysis and signalling. Nature **402:** 313–320.

Welters, P., Takegawa, K., Emr, S.D., and Chrispeels, M.J. (1994). AtVPS34, a phosphatidylinositol 3-kinase of *Arabidopsis thaliana*, is an essential protein with homology to a calcium-dependent lipid binding domain. Proc. Natl. Acad. Sci. USA **91:** 11398–11402.

Xie, Z., Nair, U., and Klionsky, D.J. (2008). Atg8 controls phagophore expansion during autophagosome formation. Mol. Biol. Cell **19:** 3290–3298.

Xue, H.W., Chen, X., and Mei, Y. (2009). Function and regulation of phospholipid signalling in plants. Biochem. J. **421:** 145–156.

Yoshimoto, K., Hanaoka, H., Sato, S., Kato, T., Tabata, S., Noda, T., and Ohsumi, Y. (2004). Processing of ATG8s, ubiquitin-like proteins, and their deconjugation by ATG4s are essential for plant autophagy. Plant Cell **16:** 2967–2983.

Zhang, Y., Li, S., Zhou, L.Z., Fox, E., Pao, J., Sun, W., Zhou, C., and McCormick, S. (2011). Overexpression of *Arabidopsis thaliana* PTEN caused accumulation of autophagic bodies in pollen tubes by disrupting phosphatidylinositol 3-phosphate dynamics. Plant J. **68:** 1081–1092.

Zhuang, X., Wang, H., Lam, S.K., Gao, C., Wang, X., Cai, Y., and Jiang, L. (2013). A BAR-domain protein SH3P2, which binds to phosphatidylinositol 3-phosphate and ATG8, regulates autophagosome formation in Arabidopsis. Plant Cell **25:** 4596–4615.